ADA038820

UNSTABLE RESONATOR THEORY

University of Arizona
Optical Sciences Center
Tucson, Arizona 85721
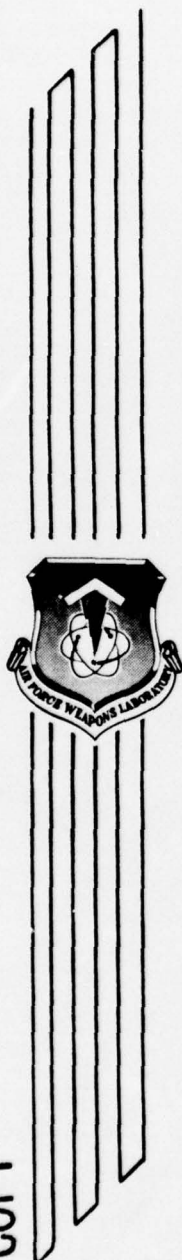
March 1977

Final Report

APR 28 1976

Approved for public release; distribution unlimited.

AD No. _____
DDC FILE COPY

AIR FORCE WEAPONS LABORATORY
Air Force Systems Command
Kirtland Air Force Base, NM 87117

This final report was prepared by the Optical Sciences Center, University of Arizona, Tucson, Arizona, under Contract F29601-75-C-0088, Job Order 317J-0199 with the Air Force Weapons Laboratory, Kirtland Air Force Base, New Mexico. Dr. P. V. Avizonis (AR) was the Laboratory Project Officer-in-Charge.

When US Government drawings, specifications, or other data are used for any purpose other than a definitely related Government procurement operation, the Government thereby incurs no responsibility nor any obligation whatsoever, and the fact that the Government may have formulated, furnished, or in any way supplied the said drawings, specifications, or other data is not to be regarded by implication or otherwise as in any manner licensing the holder or any other person or corporation or conveying any rights or permission to manufacture, use, or sell any patented invention that may in any way be related thereto.

This report has been reviewed by the Information Office (OI) and is releasable to the National Technical Information Service (NTIS). At NTIS, it will be available to the general public, including foreign nations.

This technical report has been reviewed and is approved for publication.

FOR THE COMMANDER

P. V. AVIZONIS
Technical Director, ARTO
Project Officer

DONALD L. LAMBERSON
Colonel, USAF
Chief, Advanced Radiation Technology
Office

DO NOT RETURN THIS COPY. RETAIN OR DESTROY.

REPORT DOCUMENTATION PAGE		READ INSTRUCTIONS BEFORE COMPLETING FORM
1. REPORT NUMBER AFWL-TR-76-167	2. GOVT ACCESSION NO.	3. RECIPIENT'S CATALOG NUMBER
4. TITLE (and Subtitle) UNSTABLE RESONATOR THEORY.		5. TYPE OF REPORT & PERIOD COVERED Final Report, 6. PERFORMING ORG. REPORT NUMBER
7. AUTHOR(s) M. O. Scully, G. T. Moore, R. J. McCarthy		8. CONTRACT OR GRANT NUMBER(s) F29601-75-C-0088
9. PERFORMING ORGANIZATION NAME AND ADDRESS Optical Sciences Center University of Arizona Tucson, Arizona 85721		10. PROGRAM ELEMENT, PROJECT, TASK AREA & WORK UNIT NUMBERS 626100/317J0199
11. CONTROLLING OFFICE NAME AND ADDRESS Air Force Weapons Laboratory (AP.) Kirtland Air Force Base, NM 87117		12. REPORT DATE March 1977 13. NUMBER OF PAGES 94
14. MONITORING AGENCY NAME & ADDRESS(if different from Controlling Office) 92p. 317J		15. SECURITY CLASS. (of this report) UNCLASSIFIED 15a. DECLASSIFICATION/DOWNGRADING SCHEDULE

16. DISTRIBUTION STATEMENT (of this Report)

Approved for public release; distribution unlimited.

17. DISTRIBUTION STATEMENT (of the abstract entered in Block 20, if different from Report)

18. SUPPLEMENTARY NOTES

19. KEY WORDS (Continue on reverse side if necessary and identify by block number)

Unstable Resonators
Laser Theory
Diffraction

20. ABSTRACT (Continue on reverse side if necessary and identify by block number)

This report on research on unstable resonator theory consists of three parts. Section I gives an overview of the work. In Section II a simple model is described for estimating the intensity distributions inside and emerging from lasers with high-Fresnel-number unstable resonators. In Section III modes of strip confocal unstable resonators containing spatially dependent gain are determined by means of a theory that is practical even at large Fresnel numbers.

DD FORM 1473 1 JAN 73 EDITION OF 1 NOV 65 IS OBSOLETE

402821

CONTENTS

ILLUSTRATIONS

iv

SECTION I

WORK OVERVIEW

This report summarizes work completed on unstable resonator theory for the BOA contract F29601-75-C-0088 between the Air Force Weapons Laboratory, Kirtland Air Force Base, and the University of Arizona Optical Sciences Center. The first section serves as an overview of the work. The second and third sections present preprints of two papers on unstable resonator theory to be published, probably in the Journal of the Optical Society of America.

1. Geometrical Theory of a Loaded Resonator

We have developed a simple geometrical model for estimating the intensities inside of and emerging from high-Fresnel-number unstable resonators. This model uses first-order rate equations to determine the wave amplitudes. The wavefronts are taken to be the same as in Siegman's early geometrical theory. The amplitudes in the core of the resonator (oscillator region) are found by solving a first-order differential equation along the resonator axis subject to boundary conditions on the mirrors. The amplitudes in the outer part of the resonator (amplifier region) are found by solving the rate equations in the outer region and matching their solutions to the core solution. The field is assumed to be chopped off discontinuously at the shadow boundaries. It the unsaturated gain G_o depends on the transverse coordinate, then a simple iterative procedure is used to determine the self-consistent steady-state solution. Although the predictions of the geometrical theory are crude, the theory is useful because it is simple and requires very little computer time to perform calculations. This theory is described in the preprint of Section II, "Lasers with Unstable Resonators in the Geometrical Optics Limit."

1

2. Theory Including Edge Diffraction as well as Transverse Gain Distribution

We have developed a theory that enables one to use only a small amount of computer time to calculate modes of loaded unstable resonators with sharp-edged mirrors. The theory has been developed so far only for strip (two-dimensional) resonators, but it appears that it can be generalized to resonators with rectangular mirrors in a straightforward manner. Besides the advantage of ease of computation, the theory offers other advantages over the fast Fourier transform (FFT) method. It is applicable at high effective Fresnel numbers. Indeed, it is expected to become more accurate as F_{eff} increases. Calculation for F_{eff} of several hundred is feasible. On the other hand, it also works well for low F_{eff} (near unity) provided that the magnification M is not too small. The theory can be used to calculate any of the resonator modes, not just the lowest-loss mode. However, the theory does not include effects of inhomogeneities in the index of refraction. Also, it is not clear whether an analogous theory can be developed for resonators with round mirrors.

This theory contains elements of P. Horwitz's "Asymptotic Theory of Unstable Resonator Modes,"[1] elements of our geometrical theory, and elements of Rubinowicz's line-integral approach to edge diffraction.[2] As in Horwitz's theory, the self-consistency condition on the gain is found by solving for the roots of a polynomial.

This theory is described in the preprint of Section II, "Theory of Modes in a Loaded Strip Confocal Unstable Resonator." A talk on this theory was given at Kirtland on April 26, 1976.

2

SECTION II

LASERS WITH UNSTABLE RESONATORS IN THE GEOMETRICAL OPTICS LIMIT

1. Introduction

To develop some physical understanding of the behavior of lasers with unstable resonators and to obtain numerical estimates of intensities, it is useful to consider models which are relatively simple. This treatment uses geometrical optics and rate equations to describe the single-frequency operation of a laser containing a medium with saturable gain. The treatment is valid for resonators with high effective Fresnel number. However, since diffraction of light at the mirror edges is neglected, the high-frequency low-amplitude ripples in the intensity which are found in more exact treatments[1-4] do not appear in the present theory. Also, the intensity drops to zero discontinuously at the shadow boundaries. These defects are offset by the ease with which calculations can be made using our theory. The more exact theories require time-consuming and expensive computation. Our theory allows a rapid determination of the resonator parameters which are likely to give optimal results in a more exact calculation.

In the simple case where the unsaturated gain G_o is independent of the transverse coordinates our model allows the calculation of the field distribution inside the laser by solving a first-order ordinary differential equation for the behavior in the core region and matching this to the solution of a similar equation describing the "exit rays" leaving the laser. If G_o depends on the transverse coordinates, then a simple iterative calculation can be used to determine the off-axis field. Our model is sufficiently general to describe situations where the dynamics of the active medium breaks the axial symmetry of the laser (for instance, a flowing medium). Indeed, the optical rate equations restrict the present analysis to the case where the laser and the field which it contains are axially

3

symmetric. We also neglect all refraction and diffraction and assume that the resonator is perfectly aligned. We discuss two geometries, the symmetric resonator and the confocal unstable resonator. The initial discussion is in terms of the symmetric resonator. Numerical solutions for the intensities are presented for both geometries, but with most attention being given to the confocal unstable resonator. The geometrical aspects of our treatment are based on early work of Siegman.[5] The rate equations which we use are the counterpart for the unstable resonator of equations used by Rigrod[6] to analyze one-dimensional lasers.

2. Basic Rate Equations

Siegman, in his first paper on unstable resonators[5], considered that the field inside an unstable resonator consists of two spherical waves which, for the symmetric resonator pictured in Fig. 1, emanate from virtual centers C_1 and C_2. The positions of these centers are determined by the resonator length D and the mirror curvatures. It is easy to show that this pair of waves reflect into each other if the mirrors have the form of hyperboloids with foci at C_1 and C_2. Thus, for the symmetric resonator we take the equations of the left and right mirrors to be $\rho_2 = \rho_1 + D$ and $\rho_1 = \rho_2 + D$, where ρ_1, θ_1 and ρ_2, θ_2 are spherical coordinates centered at C_1 and C_2. We make a paraxial approximation where necessary by replacing $\sin \theta_i$ by θ_i and $\cos \theta_i$ by 1. In this approximation it does not matter whether the mirrors are hyperboloidal, spherical, or whatever, as long as the mirror curvatures remain the same. The paraxial approximation is an excellent one in many cases of practical interest, but could be eliminated at the cost of increased mathematical complexity. If both mirrors of the symmetric resonator have radius a and L is the distance between C_1 and C_2, we require that the outer angle $2a/(L-D)$ of the cones of radiation emerging from the resonator be much less than one.

4

It is easy to see that if one combines two spherical waves which are solutions of the free-space Helmholtz equation, then one can match the phases of the waves on the mirrors by taking the wave vector $k = n\pi/D$. However, the amplitudes do not match. This is not surprising, since we do not expect a steady state in this case. However, we can easily match the amplitudes if we introduce a medium with a linear gain γ into the resonator and choose γ so as to just offset the geometrical losses. Then the field becomes

$$E \propto \rho_1^{-1} \exp(in\pi\rho_1/D + \gamma\rho_1) + (-1)^n \rho_2^{-1} \exp(in\pi\rho_2/D + \gamma\rho_2). \tag{1}$$

This is zero on the mirrors within the paraxial approximation if we take $\gamma = (1/D) \ln M$, where $M = (L+D)/(L-D)$ is the one-way magnification. The waves first decrease in amplitude because of geometrical spreading as one moves away from their centers and then increase in amplitude again because of the gain. In this way the amplitudes can be made to match on the mirrors.

We expect that something of this sort also happens with a nonlinear medium in the resonator. However, for the case of a nonlinear medium above threshold, the intensity adjusts itself so that the gain G equals the loss in the steady state. We anticipate that G will be a function of position and that the amplitude of the spherical waves may depend on θ_i as well as ρ_i.

To obtain the basic rate equations of our theory, we begin with the wave equation

$$\nabla^2 E = c^{-2}\partial^2 E/\partial t^2 - 2c^{-1}G\partial E/\partial t . \tag{2}$$

The saturated gain G has been put into the wave equation in the form of a negative conductivity. The gain is a function of position, but we

5

assume that the index of refraction is independent of position. This can be a valid assumption if the laser operates in the center of the gain profile. We take each spherical wave inside the laser to have the form

$$E = [f(\rho,\theta,t)/\rho]\, e^{ik\rho - i\omega t} \quad, \tag{3}$$

where $k \gg G$. The function f is assumed to be slowly varying in both space and time. If we insert Eq. (3) into Eq. (2) and put $\omega = ck$, we obtain the following equation for f:

$$\frac{\partial^2 f}{\partial\rho^2} + 2ik\,\frac{\partial f}{\partial\rho} + \frac{1}{\rho^2_\theta}\,\frac{\partial}{\partial\theta}\left(\theta\,\frac{\partial f}{\partial\theta}\right) = c^{-2}\left(\frac{\partial^2_i}{\partial t^2} - 2i\omega\,\frac{\partial f}{\partial t}\right) - 2c^{-1}G\left(\frac{\partial f}{\partial t} - i\omega f\right) . \tag{4}$$

If we neglect $\partial^2 f/\partial\rho^2$ compared to $2ik\partial f/\partial\rho$, neglect $\partial^2 f/\partial t^2$ compared to $2i\omega\partial f/\partial t$, and neglect $\partial f/\partial t$ compared to $i\omega f$, Eq. (4) reduces to the following paraxial wave equation:

$$2ik\left(\frac{\partial f}{\partial\rho} + c^{-1}\,\frac{\partial f}{\partial t} - Gf\right) + \frac{1}{\rho^2_\theta}\,\frac{\partial}{\partial\theta}\left(\theta\,\frac{\partial f}{\partial\theta}\right) = 0 \quad . \tag{5}$$

Equation (5) is sufficiently general to handle edge-diffraction effects. However, we wish to make a further approximation to Eq. (5) by dropping the term involving derivatives with respect to θ. This gives the rate equation

$$\frac{\partial f}{\partial\rho} + c^{-1}\,\frac{\partial f}{\partial t} = Gf \quad . \tag{6}$$

Equation (6) can be used to describe time-varying phenomena such as the

6

build-up of the laser field when the pumping is switched on. In the steady state $\partial f/\partial t = 0$, so that

$$\partial f/\partial \rho = Gf . \tag{7}$$

Equation (7) is the basic rate equation of our theory.

The neglect of the term in Eq. (5) containing derivatives with respect to θ represents a great simplification of the problem, but eliminates the possibility of accounting for edge-diffraction effects. The rays associated with Eq. (7) all pass through the point $\rho = 0$, and there is no possibility of ray crossing. Edge diffraction gives rise to rays which emanate from the mirror edges and bounce back and forth across the resonator, crossing in a complicated way. The wavelength dependence of the resulting diffraction pattern is conveniently parameterized in terms of the effective Fresnel number F_{eff} (also sometimes called the equivalent Fresnel number N_{eq}). One might think that for large effective Fresnel number F_{eff} (i.e., large k) this approximation would always be a good one. Actually the situation is more complicated. As k increases, the transverse oscillations in f become more and more rapid, and it is not immediately clear that the neglected term is small. Numerical calculations of Horwitz[1] show that several modes can exist within the resonator and that only the lowest-loss mode approaches the result expected from geometrical theory as $k \to \infty$. This mode does not approach the geometrical limit in a smooth manner, but rather it develops more and more rapid but smaller and smaller amplitude ripples as k increases. The phase of f is nearly constant in the resonator core even at fairly low F_{eff}, but the ripples in the modulus of f die out rather slowly as F_{eff} increases. They are about $\pm 15\%$ of the mean value for F_{eff} near 50. The magnitude of the ripples can be made less than this by using mirrors with tapered reflectivity profiles.[7,8] The calculations of Horwitz apply to resonators with rectangular-edged mirrors or to strip

7

resonators. Unfortunately no calculations for high F_{eff} resonators with round mirrors have so far been carried out. Probably the main difference to be expected with round mirrors is an increase in intensity in a region very close to the resonator axis. This increase results from constructive interference of diffracted light coming from the mirror edges. The size of the region should shrink toward zero as F_{eff} increases. In summary, it appears that Eq. (7) is valid in an average sense for the lowest-loss mode at high F_{eff}.

Figure 2 shows ray paths for the symmetric resonator. We see that the resonator is divided into two regions. In the core the left- and right-traveling rays are both present and both contribute toward saturating the gain medium. In the outer part of the resonator the "exit rays" leaving the resonator do not overlap. Let us consider the change in intensity along the exit rays. For a homogeneously broadened medium we may take G to be a function of the intensity I according to

$$G = G_0(1 + I/I_0)^{-1} ,$$ (8)

where G_0 is the unsaturated gain, which may be taken to be constant or a given function of position, and I_0 is the saturation intensity. We choose f real and normalize the field so that $I = f^2/\rho^2$. If we insert Eq. (8) into Eq. (7), we get

$$\partial f/\partial \rho = G_0 f/[1 + f^2/(I_0 \rho^2)] .$$ (9)

This equation must be solved numerically, although asymptotic properties of the solution are easily derived. For instance, if G_0 is constant and ρ is large, then

$$f \simeq (2G_0 I_0/3)^{1/2} \rho^{3/2} ,$$ (10)

8

so that the intensity increases linearly with ρ for large ρ.

3. Symmetric Resonator Intensities for the Case That G_0 Does Not Depend on r

We write the field in the symmetric resonator in the form

$$E = \rho_1^{-1} e^{ik\rho_1} f(\rho_1,\theta_1) + (-1)^n \rho_2^{-1} e^{ik\rho_2} g(\rho_2,\theta_2), \qquad (11)$$

which is a generalization of Eq. (1). The functions f and g are assumed to be slowly varying. In order that E be zero on the mirrors, we require that

$$f(\rho_1,\theta_1)/\rho_1 = g(\rho_2,\theta_2)/\rho_2 \qquad (12)$$

on the mirrors. Using the geometrical relationship between the ρ_1,θ_1 and ρ_2,θ_2 coordinates on the mirrors, Eq. (12) becomes

$$f[\tfrac{1}{2}(L+D),\theta_1] = Mg[\tfrac{1}{2}(L-D),M\theta_1], \qquad (13)$$

$$Mf[\tfrac{1}{2}(L-D),M\theta_2] = g[\tfrac{1}{2}(L+D),\theta_2]. \qquad (14)$$

These relations could be easily generalized if the mirrors were not perfectly reflecting, but had reflectivities which were functions of the radial coordinate on the mirrors.

Let us suppose that in some region suitably close to the axis it is a good approximation to assume that G_0 is independent of r. Then in this region it is consistent to assume that the field itself is independent of r, so that f does not depend on θ_1 and g does not depend on θ_2. Using Eq. (7), we have

$$df/d\rho_1 = Gf , \qquad (15)$$

$$dg/d\rho_2 = Gg . \qquad (16)$$

9

In the paraxial approximation $\rho_2 = L - \rho_1$. We take the Wronskian of Eqs. (15) and (16) by multiplying (15) by g and (16) by f and subtracting. This gives, upon integrating,

$$f(\rho_1) \, g(\rho_2) \; = \; C \, , \tag{17}$$

where C is a constant.

Using the Cartesian z coordinate shown in Fig. 1, we define f_0 and $H(z)$ by the equations

$$f[\tfrac{1}{2}(L-D) + z] \; = \; f_0 \, e^{H(z)} \, , \tag{18}$$

$$H(o) \; = \; 0 \, . \tag{19}$$

It follows from Eqs. (15) and (18) that

$$dH/dz \; = \; G \; = \; G_0/(1 + I/I_0) \, . \tag{20}$$

The total time-averaged intensity I is found from Eq. (10) to be

$$I \; = \; \rho_1^{-2} \, f^2(\rho_1) + \rho_2^{-2} \, g^2(\rho_2) - (-1)^n \, 2\rho_1^{-1} \, \rho_2^{-1} \, f(\rho_1) \, g(\rho_2)$$

$$\times \cos \, [n\pi \, (\rho_1 - \rho_2)/D] \, . \tag{21}$$

The last term is a rapidly oscillating function of position which averages to zero, and it will be neglected. We wish to write Eq. (20) as a differential equation for $H(z)$. Combining Eqs. (17), (13), (14), and (18), we have, at the left and right mirrors,

$$C \; = \; f^2 \, [\tfrac{1}{2}(L-D)] \, M \; = \; f_0^2 \, M \, , \tag{22}$$

$$C \; = \; f^2 \, [\tfrac{1}{2}(L+D)]/M \; = \; f_0^2 \, e^{2H(D)}/M \, . \tag{23}$$

10

By combining Eqs. (22) and (23), we obtain the boundary condition

$$H(D) = \ell N\ M \ . \tag{24}$$

Also, using Eqs. (18) and (22) in Eq. (17), we have

$$g[\tfrac{1}{2}(L+D) - z] = M\ f_0\ e^{-H(z)} \ . \tag{25}$$

Using Eqs. (21, (18), and (25) in Eq. (20), we obtain the desired differential equation for $H(z)$:

$$dH/dz = G_0/\{ 1 + [(\tfrac{1}{2}(L-D) + z)^{-2}\ e^{2H} + M^2(\tfrac{1}{2}(L+D) - z)^{-2}\ e^{-2H}]\ f_0^2/I_0\} \tag{26}$$

This equation must be solved subject to the boundary conditions (19) and (24). Both of these boundary conditions can be satisfied only if f_0^2/I_0 has a particular value. This value determines the steady-state intensity. Solutions exist only if the laser is above threshold ($G_0 D > \ell n\ M$).

If G_0 is independent of r for all r, then the intensities found by solving Eq. (26) are valid out to the region of the exit rays. The intensities along the exit rays may be found by matching solutions of Eq. (9) to the interior solution at the conical boundaries $\theta_i = 2a/(L-D)$ separating the interior from the exit ray region (see Fig. 2). Since the medium is less saturated in the exit ray region than in the interior, we expect the intensity to increase with angle within the exit cones out to the "cut-off" angle $\theta_i = 2a(L-D)$, where I drops to zero, as shown qualitatively in Figure 3.

In Figures 4 through 6 we show numerical solutions for the symmetric unstable resonator in which G_0 is independent of r. Here we assume that M = 2.5 and that the mirrors have equal radii. Figures 4a, 5, and 6 show the intensities I_1 and I_2 (in the core of the resonator) of the waves traveling to the right and left,

11

respectively. These are given in units of I_0 and plotted as a function of z/D. Computed points associated with I_1 and I_2 are indicated by +'s and x's respectively. Figure 4b shows the intensity on either mirror plane as a function of r/z in the domain $1 \leq r/a \leq M$. For r/a < 1 the intensity is independent of r. For r/a > M the intensity drops discontinuously to zero. Figure 4 is for the case where $G_0D = 4$ throughout the cavity. Figure 5 is for the case where $G_0D = 4$ for $D/4 < z < 3D/4$ and zero otherwise.

4. Confocal Unstable Resonator Intensities for the Case That G_0 Does Not Depend on r

The confocal unstable resonator is the configuration of choice in most applications because the output emerges in the form of a collimated beam. The geometry of the confocal unstable resonator is shown in Figure 6. The field consists of a plane wave moving to the right and a spherical wave moving to the left and centered on a point C a distance d to the right of the convex mirror. The cavity length is D. The magnification of the spherical wave in traveling from the right mirror to the left mirror is M = (D+d)/d. The left and right mirrors may be taken to be parabaloids given by the equations $\rho = z + D + d$ and $\rho = z - D + d$. The field in the cavity has the form

$$E = e^{ik(z+D+d)} f(z,r) - \rho^{-1} e^{ik\rho} g(\rho,\theta) , \qquad (27)$$

where $k = n\pi/D$. In order that E be zero on the mirrors, we require that

$$f(0,r) = (D+d)^{-1} g[D+d,r/(D+d)] , \qquad (28)$$

$$f(D,r) = d^{-1} g(d,r/d) . $$

The amplitudes f and g obey the rate equations

$$\partial f(z,r)/\partial z = Gf(z,r) , \qquad (30)$$

$$\partial g(\rho,\theta)/\partial \rho = Gg(\rho,\theta) . \qquad (31)$$

12

We assume that the concave mirror is large enough so that all of the radiation comes out to the right. If G_o is essentially independent of r in a core region suitably close to the axis, then the field may be taken to be independent of r in this core region. If the core region extends out to the cone $\theta = a/d$, which is the boundary between the interior of the laser and the exit-ray region, then the solution in the interior may be extended out to the shadow boundary $r = Ma$ by means of the exit-ray equation

$$\partial f/\partial z = G_o f/[1 + f^2/I_o] . \tag{32}$$

This equation is found by using Eqs. (30) and (8).

The differential equation giving the intensities in the core region may be derived by the same method that was used for the symmetric resonator. Taking the Wronskian of Eqs. (30) and (31), we find that

$$f(z) \, g(\rho) = C , \tag{33}$$

where C is a constant. We define H(z) and f_o by the equations

$$f(z) = f_o \, e^{H(z)} , \tag{34}$$

$$H(0) = 0 . \tag{35}$$

Combining Eqs. (33), (28), (29), and (34), we have, at the left and right mirrors,

$$C = (D+d) \, f^2(0) = (D+d) \, f_o^2 , \tag{36}$$

$$C = d \, f^2(D) = d \, f_o^2 \, e^{2H(D)} . \tag{37}$$

By combining Eqs. (36) and (37), we obtain the boundary condition

$$H(D) = \tfrac{1}{2} \ln M . \tag{38}$$

13

Note that the intensity at the right end of the cavity is a factor of M greater than the intensity at the left end. Using Eqs. (34) and (36) in Eq. (33), we have

$$g(D + d - z) = (D+d) f_0 e^{-H(z)} . \qquad (39)$$

Using Eqs. (34), (39), and (8), Eq. (30) may be written as a differential equation for $H(z)$:

$$dH/dz = g_0/\{ 1+[e^{2H} + [(D+d)/(D+d-z)]^2 e^{-2H}] f_0^2/I_0\} . \qquad (40)$$

This equation must be solved subject to the boundary conditions (35) and (38).

In Figures 7 through 10 we show numerical solutions for the confocal unstable resonator in which G_0 is independent of r. Figure 7 is for a resonator with M = 2.5 and $G_0 D = 4$. Figure 7a shows the intensities in the core, while Figure 7b shows the intensity in the plane of the convex mirror. Figures 8 and 9 are also for a resonator with M = 2.5 and $G_0 D = 4$, except that the gain medium occupies only the regions $0 < z < D/2$ and $D/4 < z < 3D/4$, respectively. Figure 10 is for a resonator with $G_0 D = 4$ everywhere, but with M = 1.5.

5. Confocal Unstable Resonator Intensities for the Case That G_0 Does Depend on r

In general it is not a good approximation to assume that G_0 is independent of r all the way out to the shadow boundaries. In this section we show how intensities in the confocal unstable resonator may be calculated for an arbitrary spatial dependence of G_0. For definiteness we assume that the core region inside of which G_0 may be considered independent of r is r < a/M. Smaller core sizes could be used without much extra work. Inside the core the solutions found in Section IV are still valid. The solutions outside the core may be found by

14

integrating the rate equations (30) and (31) along the light rays as they bounce out of the resonator, matching the intensities of the left- and right-traveling waves on the mirror planes. However, the saturated gain is a function of the intensities I_1 and I_2, which are not known until the calculation is completed. Moreover, the use of the Wronskian to cast the problem into the form of a differential equation is not possible if f depends on r and g depends on θ. We overcome this difficulty by doing an iterative calculation in which the intensities and the gain are calculated successively until both converge to a self-consistent solution. We find that this convergence occurs after about five iterations and takes very little computer time.

In order to carry out the numerical integration, I_1, I_2, G_0, and G must be evaluated on a two-dimensional grid. We use the non-uniform grid (z_m, r_n), where

$$z_m = [DM/(M-1)] (1-M^{-m/N}), \quad n = 0,\ldots,N , \tag{41}$$

$$r_n = aM^{n/N-1} , \quad n = 0,\ldots,2N . \tag{42}$$

This grid is illustrated in Figure 11 for N = 10. The advantage of this grid is that both the right- and left-traveling rays pass through the grid points, so that no interpolation is necessary. We integrate using the trapezoidal rule, stepping up one value of n at a time from the known solution in the core, first calculating I_2 and then I_1. It is possible to do the iteration at each value of n before proceeding to the next value. This would be convenient if the calculation were to be performed on a desk calculator with limited memory.

Figure 12 shows some results of calculations using our iterative scheme. We take G_0 here to depend on r according to

$$G_0 D = 4 \exp [-0.5(r/a - 0.75)^2] \tag{43}$$

for $r \geq 0.75a$. Figures 12a and 12b show the intensity on the right mirror plane,

15

assuming that M = 1.5 and M = 2.5, respectively. These results illustrate the competition between the effects of decreasing pumping at large r, which tends to decrease the intensity as r increases, and decreased saturation in the exit-ray region, which tends to increase the intensity.

6. Summary

We have described a simple geometrical model by which one can obtain intensity distributions in a high-Fresnel-number unstable resonator containing saturable gain. This model is not a substitute for the more exact, but complex, methods of calculation which include diffraction, but it does serve as a means of obtaining rough estimates of intensities in a quick, easy, and inexpensive manner.
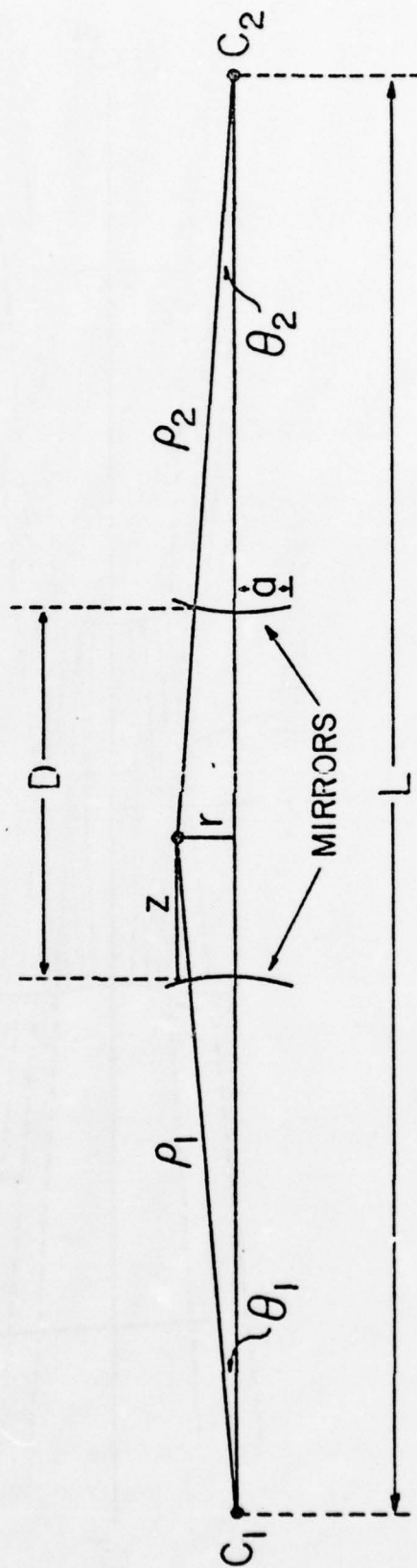
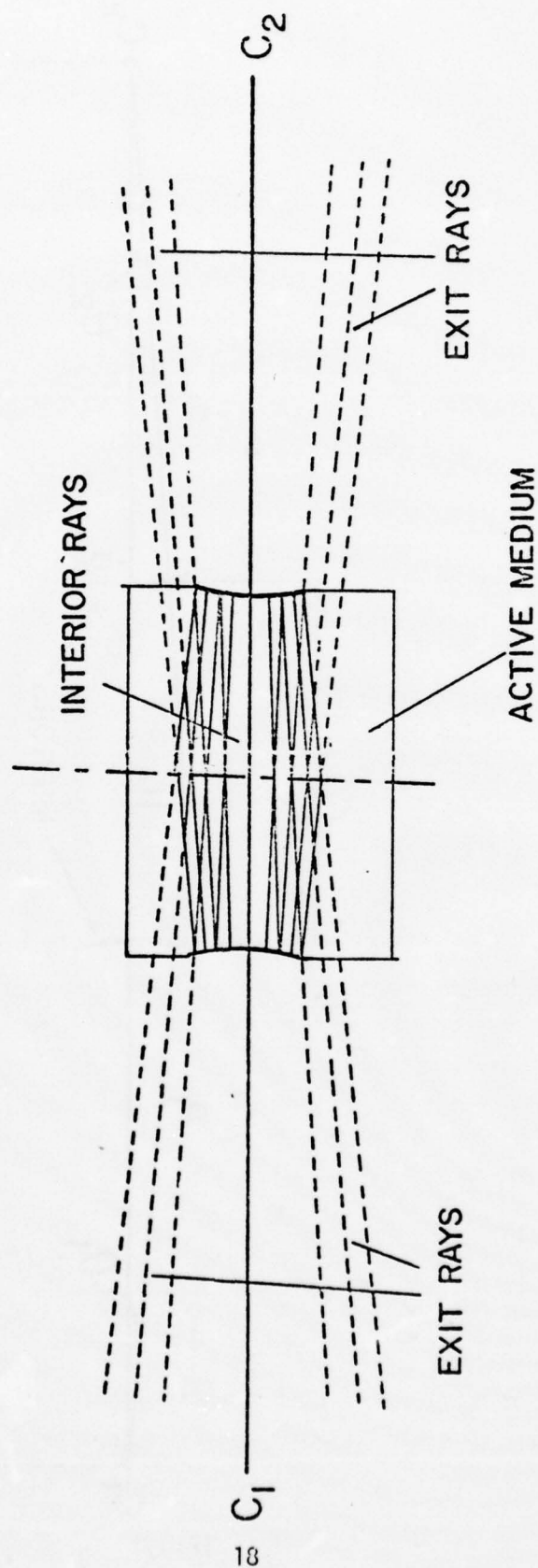Fig. 1. Geometry of the symmetric unstable resonator

Fig. 2. Interior and exit rays in the symmetric unstable resonator
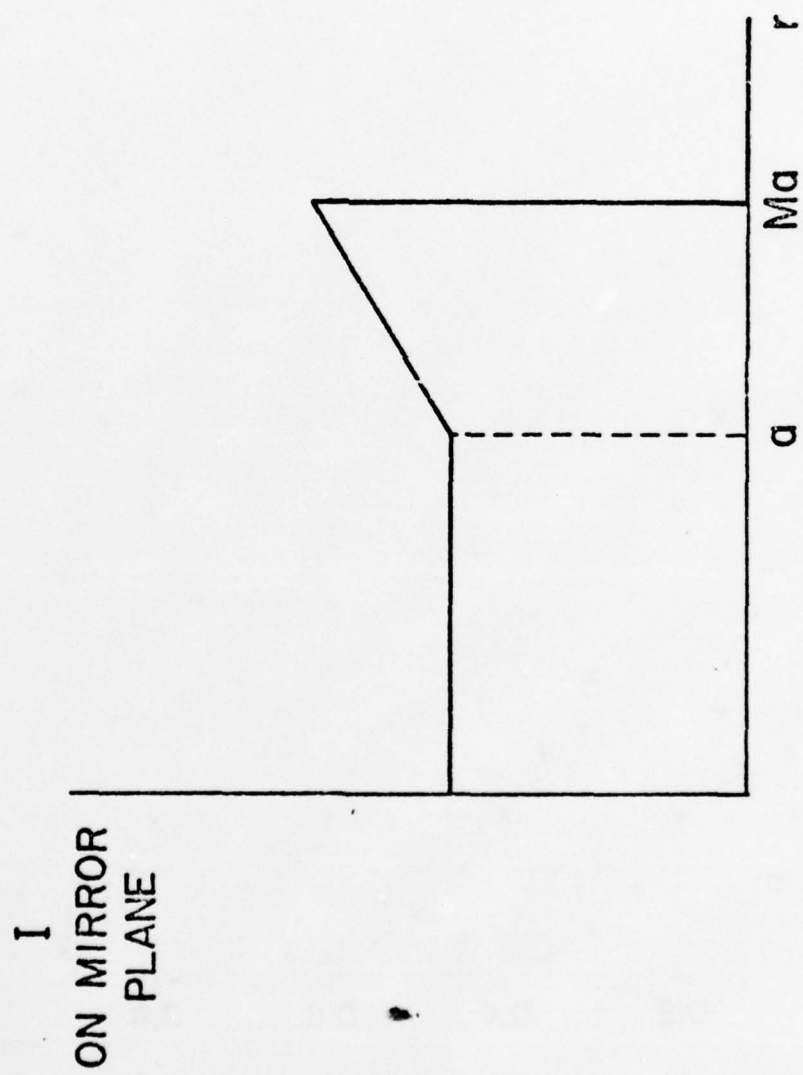
Fig. 3. Qualitative transverse dependence of intensity in the output-mirror plane in the geometrical limit
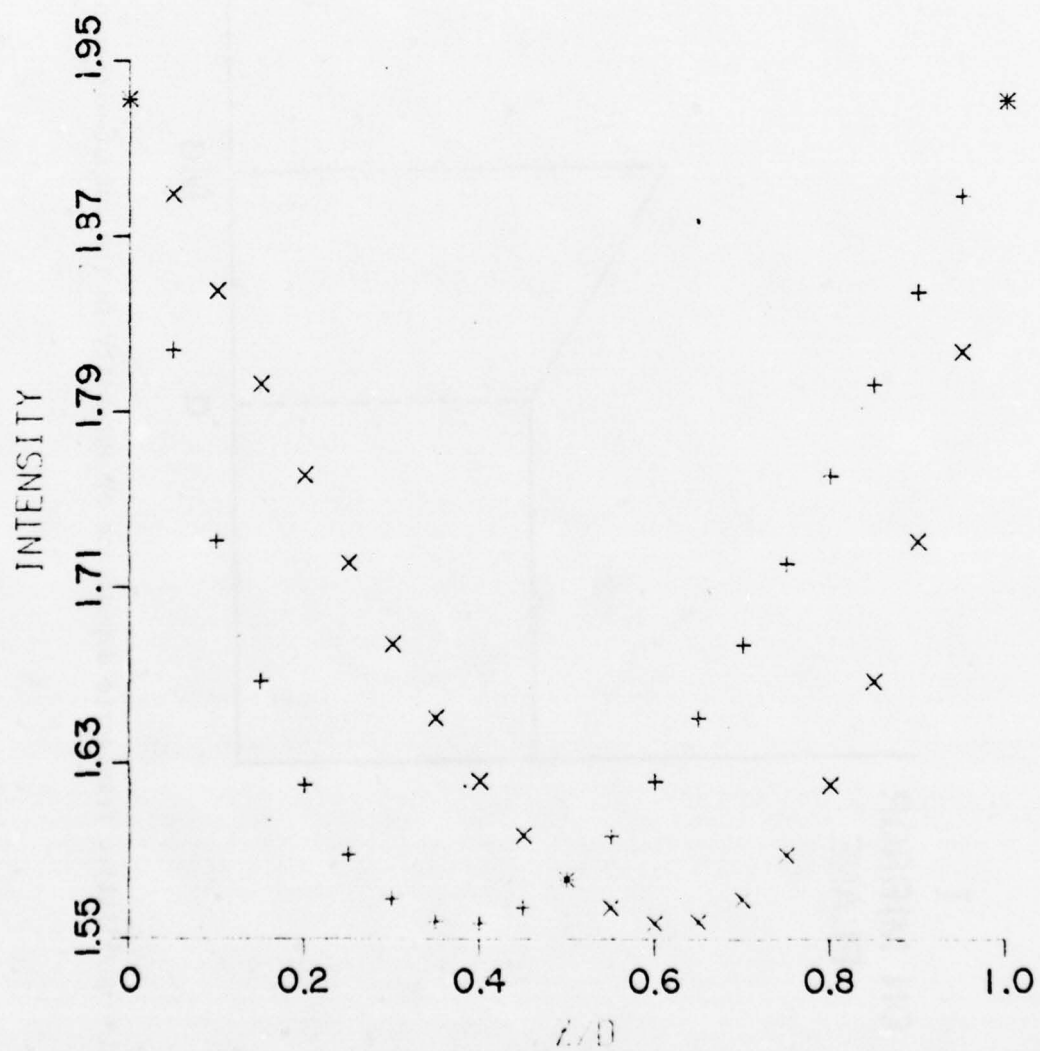
Fig. 4.a. Symmetric resonator. $M = 2.5$. $G_0D = 4$ for $0 < z < D$. On-axis symmetry
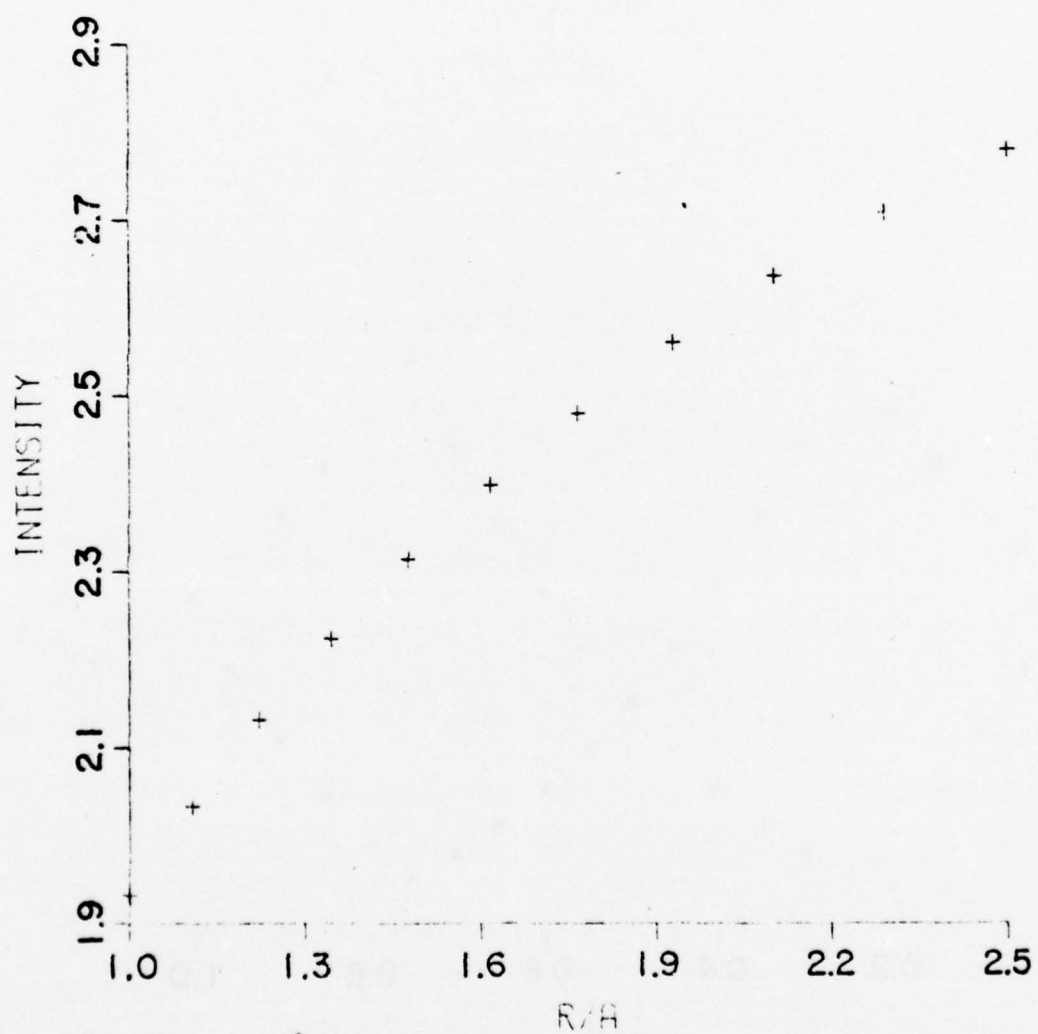
Fig.4.b. Symmetric resonator. M = 2.5. $G_oD = 4$ for $0 < z < D$. Output-mirror-plane intensity

21

Fig. 5. Symmetric resonator. $M = 2.5$. $G_0 D = 4$ for $D/4 < z < 3D/4$. On-axis intensity

22
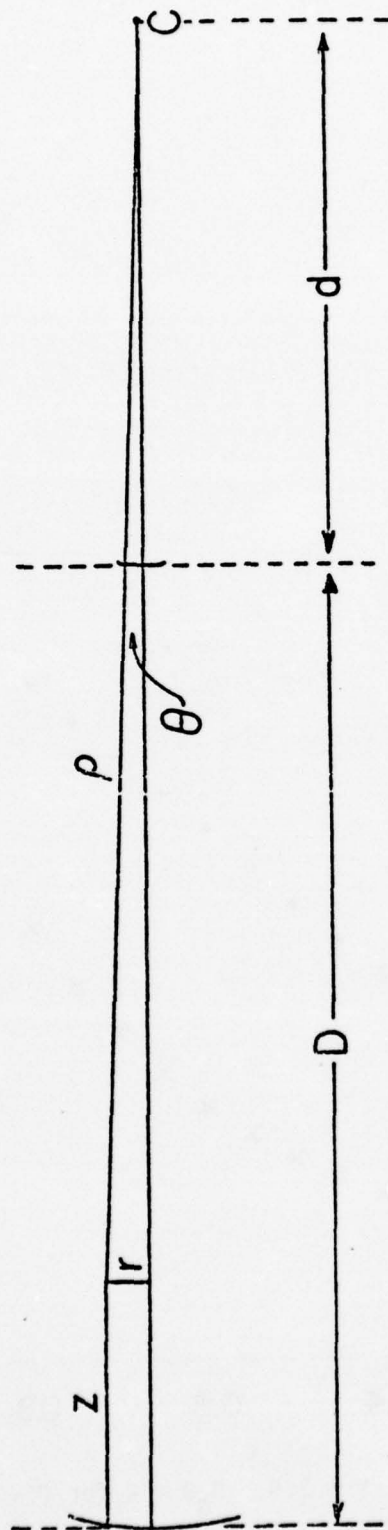
Fig. 6. Geometry of the confocal unstable resonator

23
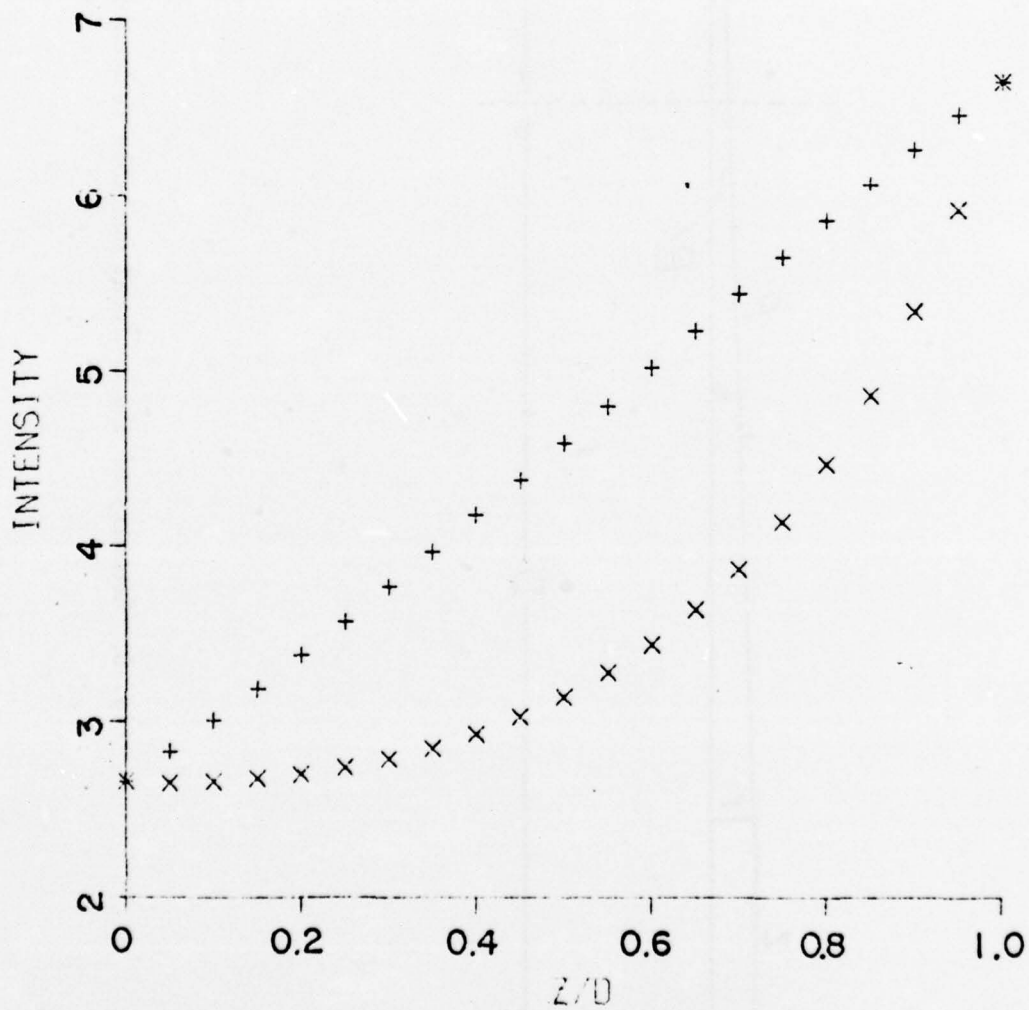
Fig. 7.a. Confocal resonator. M = 2.5. $G_0D = 4$ for $0 < z < d$. On-axis intensity

24
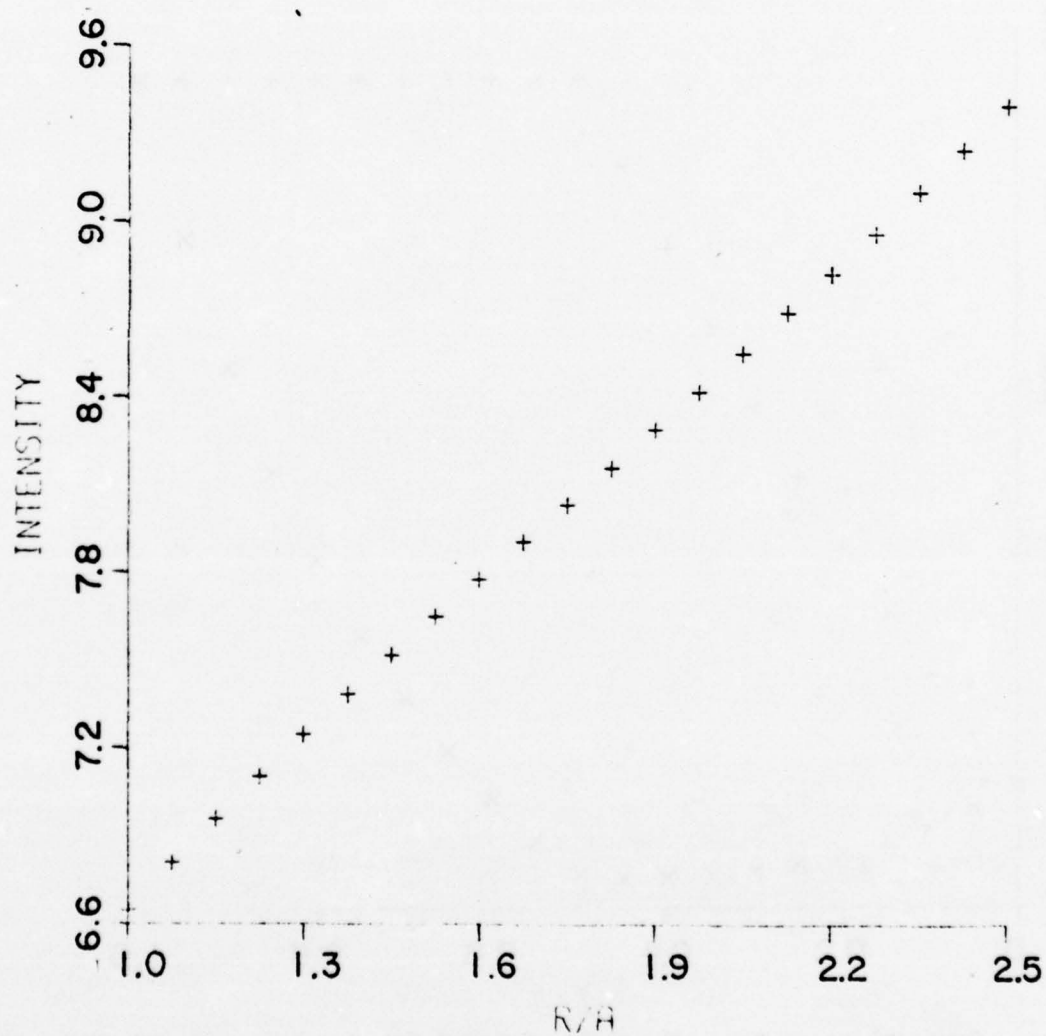
Fig. 7.b. Confocal resonator. M = 2.5. G_0D = 4 for $0 < z < d$. Output-mirror-plane intensity
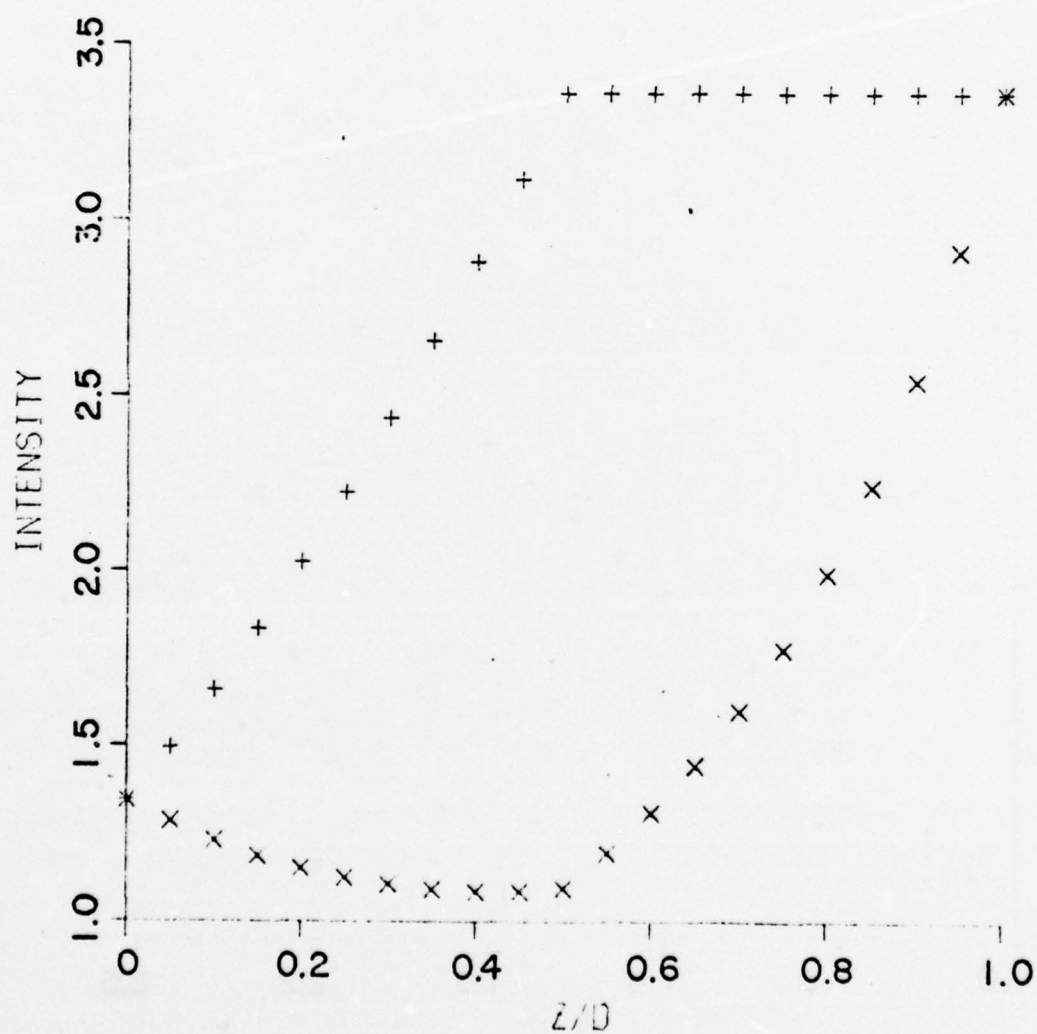
Fig. 8.a. Confocal resonator. M = 2.5. G_0D = 4 for z < D/2. On-axis intensity
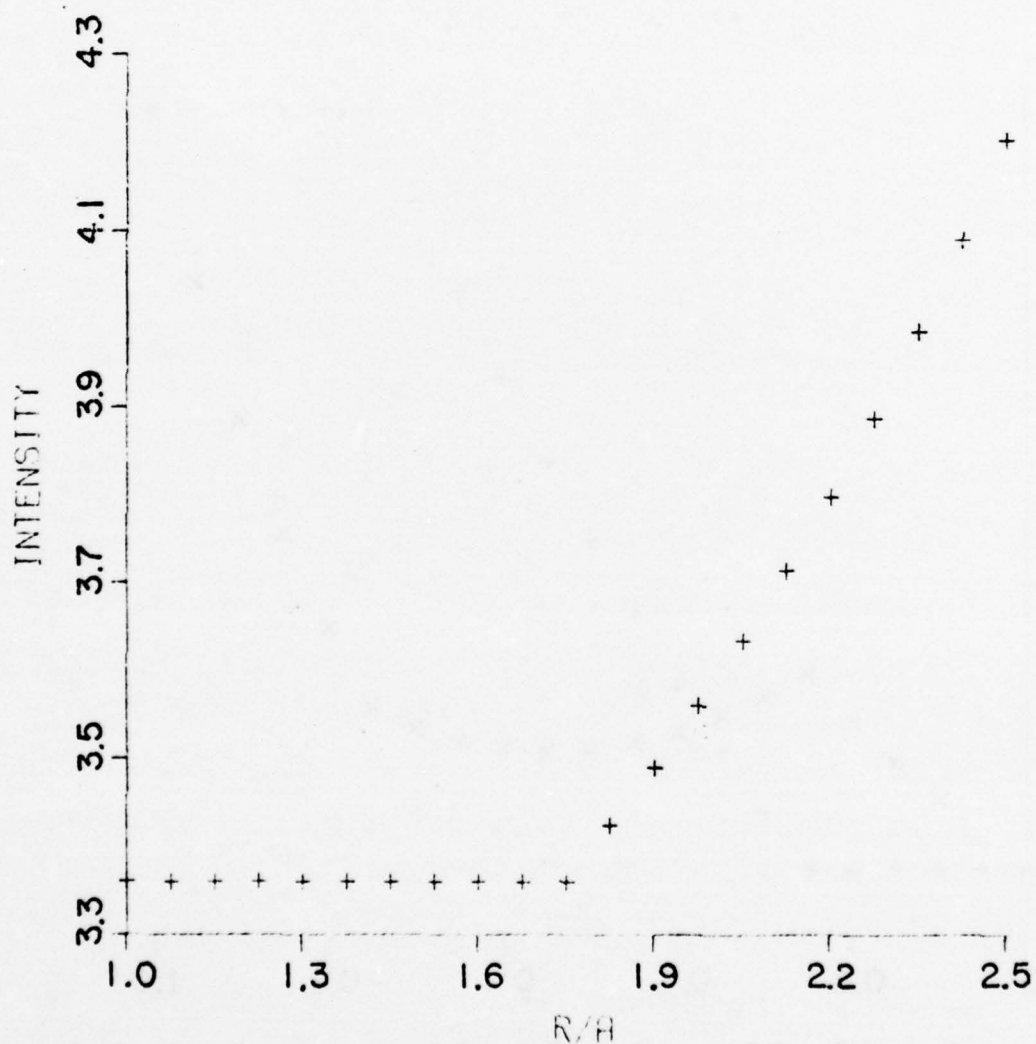
Fig. 8.b.   Confocal resonator.   M = 2.5. $G_0 D = 4$ for $z < D/2$.   Output-mirror-plane intensity
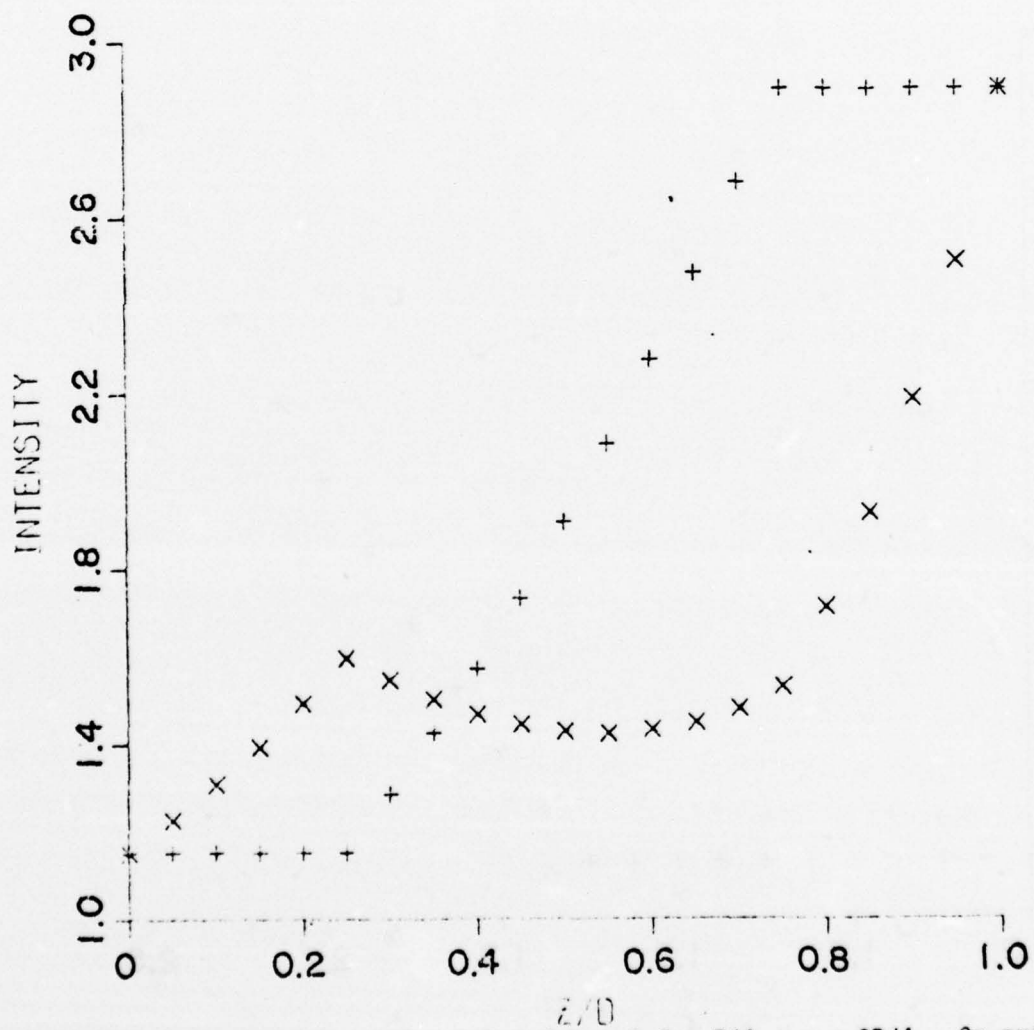
Fig. 9. Confocal resonator. $M = 2.5$. $G_0D = 4$ for $D/4 < z < 3D/4$. On-axis intensity
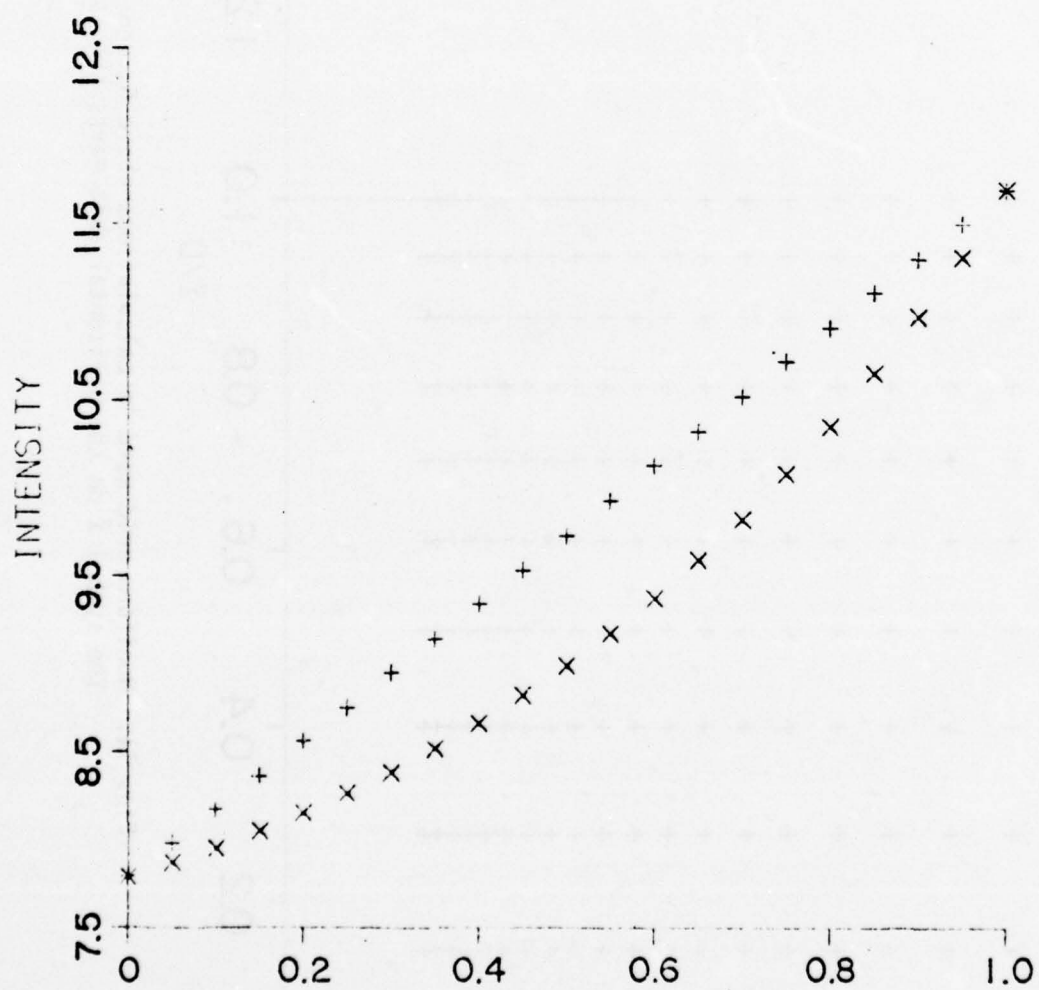
Fig. 10.   Confocal resonator.   M = 1.5. $G_0D = 4$ for $0 < z < D$.   On-axis intensity

29
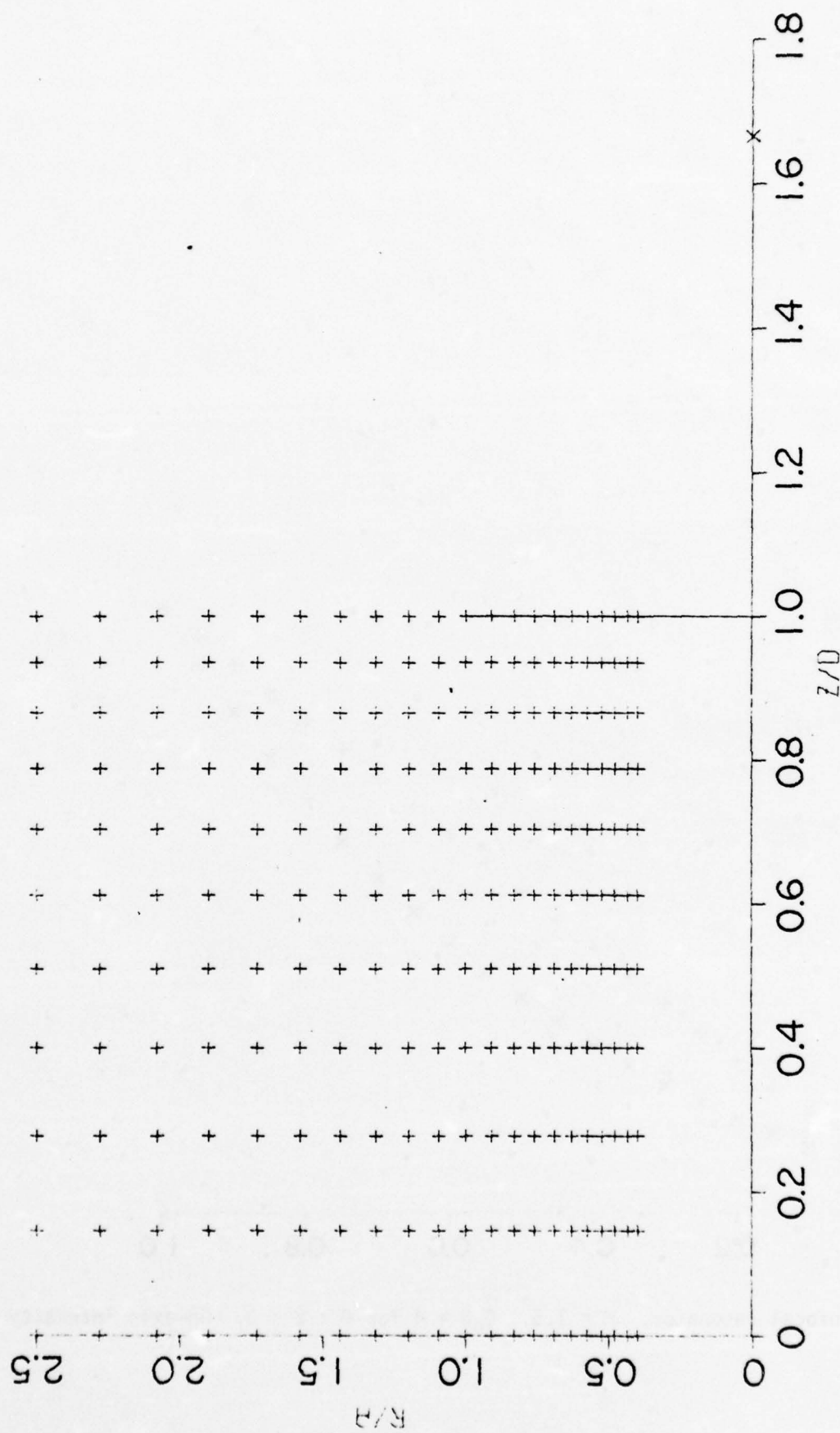
Fig. 11. Noniform grid used in calculations where f_0 depends on r. The symbol X on the horizontal axis marks the focal point
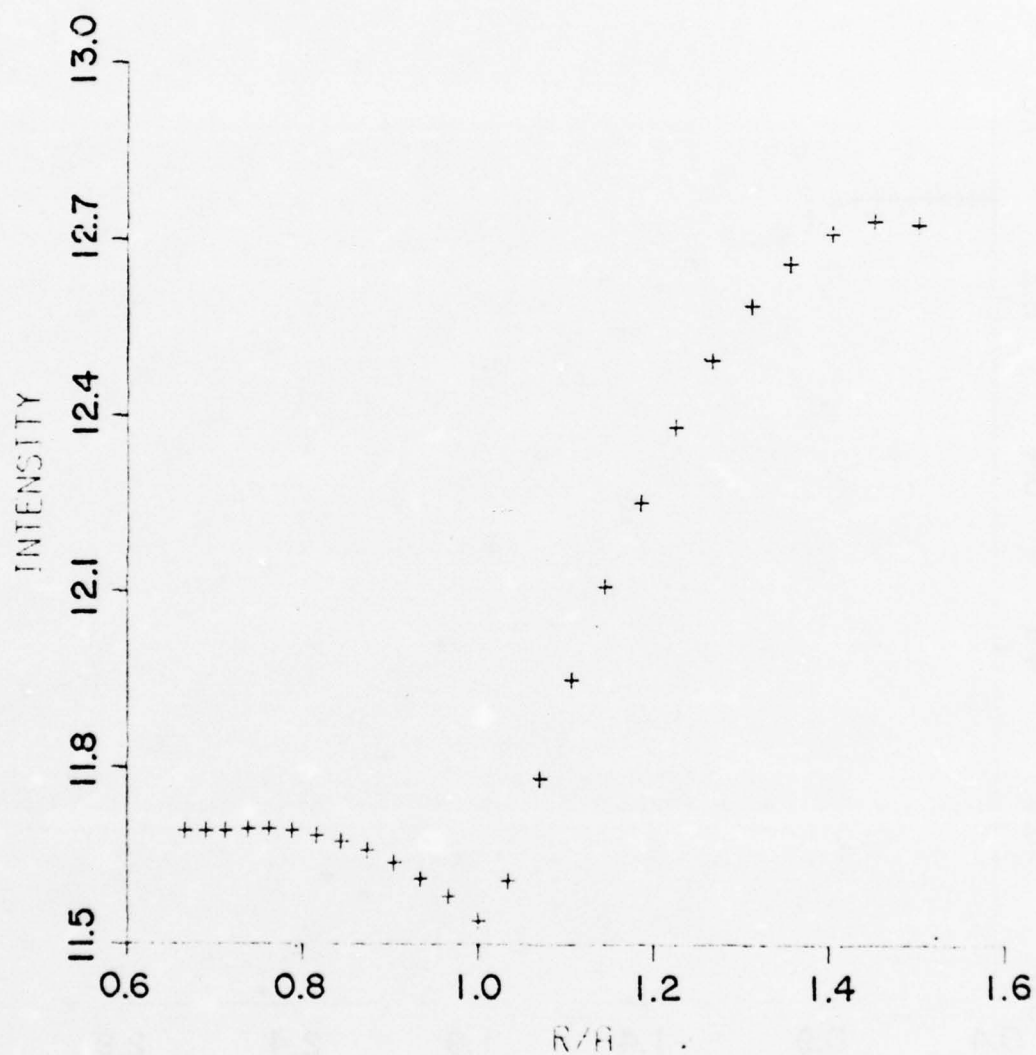
Fig. 12.a. Confocal resonator. $G_0D = 4 \exp\left[-0.5(r/a - 0.75)^2\right]$ for $r > 0.75a$. Output-mirror-plane intensity. $M = 1.5$
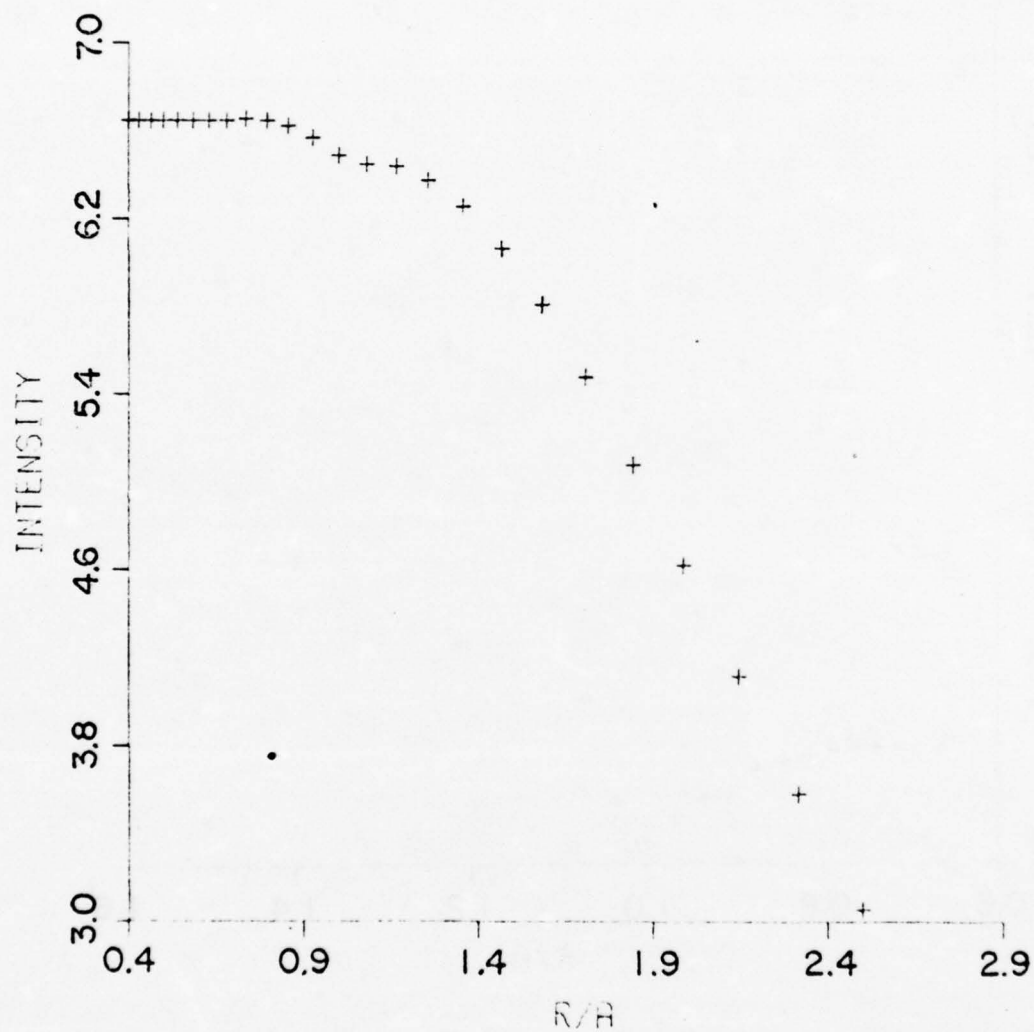
Fig. 12.b. Confocal resonator. $G_oD = 4 \exp [-0.5(r/a - 0.75)^2]$ for $r > 0.75a$. Output-mirror-plane intensity. M = 2.5

32

SECTION III

THEORY OF MODES IN A LOADED STRIP CONFOCAL UNSTABLE RESONATOR

Summary

A method is described for calculating the modes of strip confocal unstable resonators, using a technique that is practical and economical even at high Fresnel numbers. The present theory is based on work of Horwitz. In contrast to Horwitz's theory, the present theory does not give divergences at the shadow boundaries. It also applies not only to bare resonators, but to resonators in which there is arbitrary, slowly varying spatial dependence of the gain. It appears straightforward to extend the present theory to apply to three-dimensional resonators with rectangular-edge mirrors. A variety of numerical results for the symmetric modes is presented graphically.

In recent years unstable optical resonators have found wide application for high power gas lasers.[1] These resonators offer the advantages of large mode volume, automatic output coupling, and good mode control. The configuration of choice in most applications is the positive-branch confocal unstable resonator, in which the output from the resonator is in the form of a collimated beam. In performing theoretical analyses of unstable resonator modes, there are several principal difficulties. One is that, because the light emerges around the edges of at least one of the output mirrors, diffraction at the mirror edges has to be taken into account. A second factor that has to be taken into account is the transverse spatial dependence of the gain. The spatial dependence of the index of refraction also is sometimes a significant factor.

33

Theoretical determination of resonator modes generally requires computer calculations. In a geometrical theory[2] very little computer time is required, but the results are crude and not valid at low Fresnel numbers. In theories which include diffraction the costs of computing are often large or even prohibitive. Quite elaborate computer codes based on the fast Fourier transform (FFT) algorithm have been developed.[3] These codes account for diffraction, gain, and index of refraction effects, but are not practical to use at high Fresnel numbers ($F_{eff} \gtrsim 10$). Even at low Fresnel numbers it is expensive to obtain results for a sizable sample of resonator parameters. For a bare resonator several methods are available besides the FFT method. These include Fox-Li type iterative calculations[4] and matrix techniques.[5] In the matrix techniques the non-Hermitean integral equation describing the bare resonator is approximated by a matrix eigenvalue equation, and the eigenvalues and eigenfunctions are calculated numerically. The matrix techniques give the higher-loss modes in the resonator, whereas the FFT and Fox-Li methods ordinarily give only the lowest-loss mode. With these latter methods extra work is required to determine the other modes, and it is not clear how to do this for loaded resonators. None of these three methods works well at large F_{eff}.

In this paper we describe a new method of calculating modes of a strip confocal unstable resonator; i.e., a 2-dimensional resonator with cylindrical mirrors. It is well-known that the integral equation describing a 3-dimensional bare resonator with rectangular-edged mirrors can be factored into two equations for strip resonators. While this

34

factorization ordinarily is not valid for loaded resonators, it nevertheless
appears straightforward to generalize the present theory to such 3-dimensional
resonators. Our theory requires little computer time. It works efficiently for
F_{eff} in the range from about one to several hundred, provided that the magnifica-
tion M is not too close to one. It yields the high-loss modes as well as the
lowest-loss mode. Our theory is an extension of a theory of Horwitz.[6] In
contrast to Horwitz's theory, our theory does not give divergences at the shadow
boundaries. It also applies not only to bare resonators, but to resonators in
which there is arbitrary slowly varying spatial dependence of the gain. However,
at the present stage of development it does not include index-of-refraction
effects.

1. Basic Formalism

The geometry of the confocal unstable resonator is shown in Figure 13. It
consists of a concave mirror and a convex mirror aligned so as to share a common
focal point. (Actually it is a focal line in 3-space if the mirrors are cylin-
drical.) For expository purposes we take the point of view that the concave
mirror is at the left end of the cavity and the convex mirror is at the right
end of the cavity. The cavity length is D, and the focal point lies a distance
d to the right of the convex mirror. The convex mirror (also called the output
mirror) has half-size a, and the concave mirror is assumed to be large enough
to reflect virtually all of the light traveling to the left. In practical terms
a concave mirror half-size (M+1)a is sufficiently large, where M = (D+d)/d is
the resonator magnification. In geometrical theories [2,7] the light traveling
back and forth in the resonator is assumed to consist of a left-traveling cylin-
drical wave emanating from the focal point and a right-traveling plane wave.

We use two coordinate systems in our analysis. One is a Cartesian system.

This has a z coordinate which has its origin at the concave mirror and increases to the right and an x coordinate which has its origin on the resonator axis and increases upwards. The other is a polar coordinate system centered at the focal point. This has a radial coordinate ρ and an angular coordinate θ, such that points exactly to the left of the focal point have $\theta = 0$ and such that θ increases in the clockwise direction. We assume that the paraxial approximation is valid, so that in the arguments of slowly varying functions we may take

$$z = D + d - \rho , \qquad (1)$$
$$x = \theta\rho .$$

Sometimes we use a mixture of the two coordinate systems. Thus, we take the saturated gain $G(\rho,x)$ to be a slowly varying function of the longitudinal coordinate ρ and transverse coordinate x.

We consider $G(\rho,x)$ to be a given function (up to an additive function of ρ alone). The other half of the problem, that of calculating G in terms of the intensity distribution in the laser, is not treated here. A complete solution for the laser steady state could be made by iteratively calculating the intensity distribution and the gain distribution in turn until both converge to a self-consistent solution. We have applied this iterative approach to our earlier geometrical theory,[2] where we obtain convergence after about five iterations. Since the main objective in our present work has been to test the validity of our approach in a simple 2-dimensional geometry before proceding to a 3-dimensional theory, we have not considered it worthwhile to do an iterative calculation for the strip resonator. We assume that the gain is symmetric,

36

$G(\rho,x) = G(\rho,-x)$, so that the resonator modes are either symmetric or anti-symmetric. Also, we assume that the mirrors are perfectly aligned and perfectly reflecting. We take the field E to obey the scalar Helmholtz equation.

The effective Fresnel number is given by

$$F_{eff} = a^2 k/(4\pi d) , \tag{3}$$

where k is the wave vector. This parameter is called the equivalent Fresnel number (N_{eq}) by some authors.[1,3,4,5] Resonator mode losses are well-known to exhibit a quasi-periodicity in F_{eff}, such that single-mode operation is favored near half-integral values of F_{eff}.

We write the field in the cavity in the form

$$E = f(z,x) \exp [ik(z+Md)] - \rho^{-\frac{1}{2}} g(\rho,\theta) e^{ik\rho} . \tag{4}$$

The optical phases match on the mirror surfaces. If we use Eq. (4) in the Helmholtz equation, we obtain the following paraxial equations for f and g:

$$2ik (\partial f/\partial z - Gf) + \partial^2 f/\partial x^2 = 0 , \tag{5}$$

$$2ik (\partial g/\partial \rho - Gg) + \rho^{-2}\partial^2 g/\partial \theta^2 = 0 . \tag{6}$$

Also, since E must be zero on the mirrors, we obtain from Eq. (4) the boundary conditions

$$f(0,Md\theta) = (Md)^{-\frac{1}{2}} g(Md,0) , \tag{7}$$

$$g(d,\theta) = \begin{cases} d^{\frac{1}{2}}f(D,d\theta) e^{2ikD} , & |\theta| < a/d , \\ 0 , & |\theta| > a/d . \end{cases} \tag{8}$$

Before discussing the effects of diffraction, we examine briefly how our geometrical theory[2] applies to the strip resonator. Our geometrical theory is obtained by neglecting the last terms on the left-hand sides of Eqs. (5) and (6). This gives the rate equations

$$\partial f/\partial z = Gf \quad , \tag{9}$$

$$\partial g/\partial \rho = Gg \quad . \tag{10}$$

Note that we define the gain G as a logarithmic derivative of amplitudes, rather than intensities. The logarithmic derivative of intensities is obviously 2G. It turns out that, if F_{eff} is large, the effect of diffraction simply adds a low-amplitude high-frequency ripple to the geometrical solution. Sufficiently close to the axis it is consistent with the geometrical theory to regard G, f, and g as independent of x and θ. Setting $x = \theta = 0$ and taking the Wronskian of Eqs. (9) and (10), one obtains

$$f(0,0) \, g(Md,0) = f(D,0) \, g(d,0) \quad . \tag{11}$$

Using Eqs. (7) and (8) in Eq. (11) gives

$$e^{2ikD} \, M^{-\frac{1}{2}} g^2(Md,0) = g^2(d,0) \quad . \tag{12}$$

Comparing Eq. (12) with the solution of Eq. (10) ,

$$g(\rho,0) = g(d,0) \, \exp[\int_d^\rho G(\rho',0) \, d\rho'] \quad , \tag{13}$$

38

for $\rho = Md$, we obtain

$$\mu = 1 \quad , \tag{14}$$

where

$$\mu \equiv M^{-\frac{1}{2}} e^{2ikD} \exp[2 \int_d^{Md} G(\rho',0) \, d\rho'] \quad . \tag{15}$$

Thus, gain distributions which are consistent with a steady state in the cavity must satisfy Eq. (14). If we include the effects of diffraction, Eq. (14) is no longer valid. We shall show that Eq. (14) may be replaced to a good approximation by the condition that μ be the root of a polynomial.

Let us define

$$Q \equiv \int_d^{Md} G(\rho',0) \, d\rho' \quad . \tag{16}$$

Also, let

$$G(\rho,x) = Q/D + G'(\rho,x) \quad . \tag{17}$$

We regard $G'(\rho,x)$ as a given function. The integrated gain of G' along the axis is zero. Q cannot be specified beforehand, but must be calculated from the theory; Q is known once μ has been determined. It turns out that in order to calculate the field on the output-mirror plane, only the integral of G' along various rays traversing the resonator need be known. Thus, there are many gain distributions G' which give the same field on the output-mirror plane. For instance, if we add to G' any

39

function of ρ alone whose integral over the cavity is zero, then the integrated gain is unaffected.

In this paper we assume that the laser operates at steady state with a single frequency. However, the case where $G' \equiv 0$ is mathematically equivalent to the case of decaying modes in a bare resonator. We accordingly refer to a laser having $G' \equiv 0$ as a bare resonator, even though we understand that G cannot be zero if a steady state exists.

If we wish to account for the effects of diffraction at the mirror edges, it is not possible to neglect the second derivatives in Eqs. (5) and (6). Diffracted rays emanate from the mirror edges and bounce back and forth across the cavity. The phases associated with these rays have rapid transverse oscillations. If one looks at the field associated with these rays well inside the geometrical shadow boundaries, then the field, aside from slowly varying amplitudes, consists of cylindrical waves emanating from the mirror edges and the virtual images of the mirror edges. These image points $(\rho_n, \pm x_n)$ are given by the equations

$$\rho_n = dM^{2n} , \qquad (18)$$

$$x_n = aM^n , \qquad (19)$$

where n takes on all integral values. Clearly these points lie on a parabola. For $n < 0$ the points lie to the right of the cavity, for $n = 0$ the points are the output mirror edges, and for $n > 0$ the points lie to the left of the cavity (see Fig. 14) if we wish to calculate E out to the region of the shadow boundaries and beyond, then the two points for $n = 0$ are to be regarded as edges of an aperture illuminated by cylindrical waves coming from the image points for which $n < 0$. Similarly the two points for $n = 1$ are to be regarded as edges of

of an aperture illuminated by cylindrical waves emanating from the image points for which n > 1.

In accordance with the above discussion, we write the amplitudes f and g appearing in Eq. (4) in the form

$$f(z,x) = \sum_{n=1}^{N} (\rho_n - \rho)^{-\frac{1}{2}} [\exp\{i\frac{k}{2}(x-x_n)^2/(\rho_n-\rho)\} f_n(\rho,x)$$

$$\pm \exp\{i\frac{k}{2}(x+x_n)^2/(\rho_n-\rho)\} f_n(\rho,-x)] + \hat{f}(\rho,x) \quad , \quad (20)$$

$$\rho^{-\frac{1}{2}}g(\rho,\theta) = \sum_{n=0,-1,-2,\ldots}^{-N+1} (\rho-\rho_n)^{-\frac{1}{2}} [\exp\{i\frac{k}{2}(\theta-x_n/\rho_n)^2/(-\frac{1}{\rho} + \frac{1}{\rho_n})\}$$

$$x \, g_n(\rho,x) \pm \exp\{i\frac{k}{2}(\theta + \frac{x_n}{\rho_n})^2/(-\frac{1}{\rho} + \frac{1}{\rho_n})\} g_n(\rho,-x)]$$

$$+ \rho^{-\frac{1}{2}}\hat{g}(\rho,x) \quad . \quad (21)$$

It is consistent with edge diffraction effects to take f_n, $\hat{f}$, g_n, $\hat{g}$ to be slowly varying functions, whereas f and g have rapid oscillations, particularly at large F_{eff}. Our chief objective is to calculate $f(D,x)$.

The phases appearing in Eqs. (20) and (21) are the Fresnel approximation to the phases of cylindrical waves emanating from points $(\rho_n, \pm x_n)$. These phases are rapidly oscillating if $|n|$ is small, but approach the constant phase

$$\exp(ika^2/2d) = \exp(2\pi i F_{eff}) \quad (22)$$

41

as $|n|$ becomes large. The number N is to be chosen large enough so that this limit has essentially been reached when $|n| = N$. (Horwitz finds that taking $M^N = 250\ F_{eff}$ gives a sufficiently large value of N.) Thus, we have rays which emanate from the mirror edges and make N round trips of the cavity. The rays associated with $\hat{f}$ and $\hat{g}$, on the other hand, originate in the core, as do the rays of our geometrical theory. Equations (20) and (21) are supposed to apply well inside the shadow boundaries. The way in which these equations are modified to apply in the outer part of the resonator is described later. The $\pm$ signs refer to the symmetric and antisymmetric modes.

It is fairly obvious [and may be verified by inserting the terms of Eqs. (20) and (21) into Eqs. (5) or (6)] that, provided G is slowly varying, the amplitudes f_n, $\hat{f}$, g_n, $\hat{g}$ all obey rate equations of the form

$$\frac{\partial f_n}{\partial s} = G\ f_n\ , \quad \frac{\partial g_n}{\partial s} = G\ g_n\ , \quad \text{etc.} \quad , \tag{23}$$

where $\partial/\partial s$ indicates the directional derivative along the direction of ray propagation.

Besides the rate equations, we need to specify the boundary conditions satisfied by the various amplitudes. The boundary conditions at the concave mirror are easily found by setting $\rho = Md$ and $\theta = x/(Md)$ in Eqs. (20) and (21) and equating coefficients of like exponentials when these expressions for f and g are used in Eq. (7). This gives

$$(\rho_n - Md)^{-\frac{1}{2}} f_n(Md,x) = (Md - \rho_{1-n})^{-\frac{1}{2}} g_{1-n}(Md,x)\ ,$$

$$n = 1,2,\ldots,N\ , \tag{24}$$

$$\hat{f}(Md,x) = (Md)^{-\frac{1}{2}} \hat{g}(Md,x) \quad . \tag{25}$$

The boundary conditions at the right end of the cavity require more care. The total field must vanish on the mirror, whereas the left traveling part of the field must vanish for $|x| > a$. Let us suppose that $G = 0$ in a region just inside the right end of the cavity. This assumption is made for mathematical convenience, and our final results probably do not depend on it. With this assumption $g(\rho,\theta)$ can be given for ρ near the right end of the cavity in terms of $g(d,\theta)$:

$$g(\rho,\theta) = \frac{1}{2\pi} \left[2ik\pi/(\frac{1}{\rho} - \frac{1}{d})\right]^{\frac{1}{2}}$$

$$x \int d\theta' \, g(d,\theta') \, \exp\left[\frac{k}{2i} (\theta-\theta')^2/(\frac{1}{\rho} - \frac{1}{d})\right] \quad . \tag{26}$$

Using Eq. (8) in Eq. (26) and setting $\eta = \theta'd/a$, we get

$$g(\rho,\theta) = \frac{1}{2\pi} \left[2ik\pi/(\frac{1}{\rho} - \frac{1}{d})\right]^{\frac{1}{2}} \, ad^{-\frac{1}{2}} \, e^{2ikD}$$

$$x \int_{-1}^{1} d\eta \, f(D,a\eta) \, \exp\left[\frac{k}{2i}(\theta - a\eta/d)^2/(\frac{1}{\rho} - \frac{1}{d})\right] \quad . \tag{27}$$

The correct sign of the square root is that for which the real part is positive. We insert the specific form of $f(D,a\eta)$ in Eq. (20) and carry out the integration over η using an approximate formula developed in the appendix of Horwitz's paper. For our purposes this formula can be written in the form

43

$$
\begin{aligned}
I &\equiv \int_{-1}^{1} \exp\left[i(A\eta^2 - 2B\eta + C)\right] \; F(\eta) \; d\eta \\[2mm]
&\simeq (i\pi/A)^{\frac{1}{2}} \; F(B/A) \exp\left[i(C - B^2/A)\right] \\[4mm]
&\quad + F(-1) \left[2i(A + B)\right]^{-1} \exp\left[i(A + 2B + C)\right] \\[4mm]
&\quad + F(1) \left[2i(A - B)\right]^{-1} \exp\left[i(A - 2B + C)\right] \quad .
\end{aligned}
$$

$$(28)$$

In Eq. (28) it is assumed that A and B are large and that B/A lies in the domain of integration and not close to $\eta = \pm 1$. It is also assumed that $F(\eta)$ is slowly varying. Physically, the first term on the right hand side of Eq. (28) corresponds to reflection and the other two terms correspond to diffracted light emitted from the mirror edges. Equation (28) becomes singular if $A = \pm B$. These singularities are at the positions of the geometrical shadow boundaries. The singularities in Eq. (28) can be readily eliminated, as we show later. However, for now we restrict our attention to points well inside the shadow boundaries.

Once the integration over η in Eq. (27) has been carried out and the form of $g(\rho,\theta)$ in Eq. (21) has been substituted for the left hand side of Eq. (27), the slowly varying functions multiplying the various rapidly oscillating exponentials are equated term by term. After a certain amount of algebra one obtains the following results:

The functions f_n, $\hat{f}$, g_n, $\hat{g}$ obey the boundary conditions which one would expect on the basis of geometrical optics.

$$e^{2ikD} (\rho_n - d)^{-\frac{1}{2}} f_n(d,x) = (d - \rho_{-n})^{-\frac{1}{2}} g_{-n}(d,x) ,$$

$$\tag{29}$$

$$n = 1, \ldots, N-1 ,$$

$$e^{2ikD} \cdot \{(\rho_N - d)^{-\frac{1}{2}} \exp (ika^2/2d) [f_N(d,x) \pm f_N(d,-x)] + \hat{f}(d,x)\}$$

$$\tag{30}$$

$$= d^{-\frac{1}{2}} \hat{g}(d,x) .$$

The last two terms on the right hand side of Eq. (28) lead to an expression for $g_0(\rho,x)$, the amplitude of the diffracted wave on its first trip across the cavity. This expression is only correct near the output mirror and must be multiplied by the exponential of the gain integral according to Eq. (23) in order to be valid over the whole length of the cavity. One obtains

$$g_0(\rho,a+(\rho-d)\alpha) = -e^{2ikD} (i/2\pi k)^{\frac{1}{2}} \{\sum_{n=1}^{N} (\rho_n - d)^{-\frac{1}{2}}$$

$$\times [\exp \{i\tfrac{k}{2}(x_n-a)^2/(\rho_n-d)\} f_n(d,a) (\alpha_n^{(+)} - \alpha)^{-1}$$

$$\tag{31}$$

$$\pm \exp \{i\tfrac{k}{2}(a+x_n)^2/(\rho_n-d)\} f_n(d,-a) (\alpha_n^{(-)} - \alpha)^{-1}]$$

$$+ \hat{f}(d,a) (a/d - \alpha)^{-1}\} \exp [\int_d^\rho G(\rho',a+(\rho'-d)\alpha) \, d\rho'] .$$

In this equation α is the angle with respect to the axis of the ray from the mirror edge at (d,a) to the point where g_0 is evaluated. Thus, if the ray hits the concave mirror at position x_f, then $\alpha = (x_f-a)/[d(M-1)]$. The angles $\alpha_n^{(\pm)}$ are the angles with respect to the axis of rays emanating

45

from the points $(\rho_{-n}, \pm x_{-n})$ and striking the output mirror edge at (d,a). Specifically, $\alpha_n^{(\pm)} = (a/d)(1 \pm M^{-n})^{-1}$. These are just the angles of the shadow boundaries. These angles rapidly approach a/d as n becomes large if M is not close to one. These shadow boundaries are illustrated in Figure 2.

Equation (31) describes the propagation of the amplitude of the diffracted wave on its first trip across the cavity. By solving Eq. (23) and applying the boundary conditions (24) and (29) the diffracted wave may be propagated through N round trips across the cavity. The solutions of Eq. (23) are

$$f_n(Md-z, x-(x-x_n)z/(Md-\rho_n)) = f_n(Md,x)$$

$$\times \exp\left[\int_0^z dz' \, G(Md-z', x-(x-x_n)z'/(Md-\rho_n))\right], \quad n = 1,\ldots,N ,$$

(32)

$$g_n(\rho, x+(\rho-d)(x-x_n)/(d-\rho_n)) = g_n(d,x)$$

$$\times \exp\left[\int_d^\rho G(\rho', x+(\rho'-d)(x-x_n)/(d-\rho_n)) \, d\rho'\right], \quad n = -1,-2,\ldots,-N+1 .$$

(33)

If we were to make an iterative calculation in which G had to be determined in terms of the intensities in the cavity, then we would need to evaluate f_n and g_n throughout the cavity (on a suitable grid). However, for the present purposes we concentrate our attention on the amplitudes $f_n(d,x)$, $\hat{f}(d,x)$ from which the right-traveling field of the laser can be determined on the output mirror plane, according to Eqs. (4), (20) and (21). If we set $z = D$ in Eq. (32) and $\rho = Md$ in Eq. (33) and apply the boundary

conditions (24) and (29), then $f_n(d,x)$ can be expressed in terms of $f_1(d,x)$ by the equation

$$f_n(d,x) = e^{2i(n-1)kD} M^{(n-1)/2} [\Gamma_n(x)/\Gamma_1(s_n(x))] f_1(d,s_n(x)) , \qquad (34)$$

where

$$s_n(x) = \frac{1-M^{-2}}{1-M^{-2n}} M^{1-n} x + \frac{M^{-1}-M^{1-2n}}{1-M^{-2n}} a . \qquad (35)$$

In Eq. (34) we have introduced the function $\Gamma_n(x)$, which is defined as the exponential of the integrated gain along a ray which leaves the edge of the output mirror at point (d,a), makes n round trips across the cavity and hits the output mirror plane at point (d,x). Explicitly $\Gamma_n(x)$ is given by the formula

$$\Gamma_n(x) = \exp \{ \sum_{m=1}^{n} [\int_d^{Md} G(\rho', \frac{M^{1-m}}{1-M^{-2n}} (-M^{-n}x + a)$$

$$+ \frac{\rho'}{d} \frac{M^{-1-n+m}}{1-M^{-2n}} (x-M^{-n}a)) d\rho' + \int_d^{Md} G(\rho', \frac{M^{-n+m}}{1-M^{-2n}} (x-M^{-n}a)$$

$$\qquad (36)$$

$$+ \frac{\rho'}{d} \frac{M^{-m}}{1-M^{-2n}} (-M^{-n}x + a)) d\rho'] \} .$$

The first integral in Eq. (36) gives the integrated gain on the m'th trip to the left; the second integral gives the integrated gain on the m'th trip to the right. If we examine the ray paths given in Eq. (36), we see that those rays which remain in the resonator for many bounces enter and leave the core along paths nearly antiparallel or parallel to the

47

rays of the geometrical theory. All except the first and last few trips take place close to the axis.

We define $\Gamma_n'(x)$ in the same way as $\Gamma_n(x)$, except that G' is to be substituted for G in Eq. (36). Then

$$\Gamma_n(x) = e^{2nQ} \, \Gamma_n'(x) \quad . \tag{37}$$

Also note that

$$\mu = M^{-\frac{1}{2}} \, e^{2Q+2ikD} \quad . \tag{38}$$

The functions $\Gamma_n'(x)$ converge to a limit function as n becomes large, since rays very close to the axis do not contribute significantly to the gain integrals. This convergence is the principal reason for defining G' as we do.

We can relate $f_1(d,x)$ to $f_n(d,\pm a)$ by starting with Eq. (31) and making one round trip of the cavity. This gives

$$
\begin{aligned}
f_1(d,x) = & -e^{2ikD} \, M^{\frac{1}{2}} \, \Gamma_1(x) \, (i/2\pi k)^{\frac{1}{2}} \, \{ \sum_{m=1}^{N} d^{-\frac{1}{2}} (M^{2m}-1)^{-\frac{1}{2}} \\
& \times [\exp'\{\frac{ika^2}{2d} \frac{1-M^{-m}}{1+M^{-m}}\} \, f_m(d,a) \, (\frac{a}{d} \frac{1}{1+M^{-m}} - \frac{xM^{-1}-aM^{-2}}{d(1-M^{-2})})^{-1} \\
& \pm \exp'\{\frac{ika^2}{2d} \frac{1+M^{-m}}{1-M^{-m}}\} \, f_m(d,-a) \, (\frac{a}{d} \frac{1}{1-M^{-m}} - \frac{xM^{-1}-aM^{-2}}{d(1-M^{-2})})^{-1}] \\
& + \hat{f}(d,a) \, (\frac{a}{d} - \frac{xM^{-1}-aM^{-2}}{d(1-M^{-2})})^{-1} \} \quad .
\end{aligned}
\tag{39}
$$

48

Inspection of Eq. (39) reveals that the major part of the x dependence of $f_1(d,x)$ is of the form $\Gamma_1(x)/(a - x/M)$. Accordingly, if we define $q(x)$ by

$$f_1(d,x) = e^{2ikD} M^{\frac{1}{2}} \Gamma_1(x) q(x)/(a-x/M) \quad , \tag{40}$$

then $q(x)$ will be nearly constant. Setting $x = \pm a$ in Eq. (34), substituting into the righthand side of Eq. (39), and using Eq. (40), we obtain

$$
\begin{aligned}
q(x) = &-(id/2\pi ka^2)^{\frac{1}{2}} \{ \sum_{m=1}^{N} (M^{2m}-1)^{-\frac{1}{2}} [\exp'\{\frac{ika^2}{2d} \frac{1-M^{-m}}{1+M^{-m}}\} \\
& \times e^{2imkD} M^{m/2} \Gamma_m(a) q(\frac{M^{-1}+M^{1-m}}{1+M^{-m}} a) \\
& \times (1+M^{-m}) (1 - \frac{aM^{-m}(1-M^{-2})}{(1+M^{-m})(a-x/M)})^{-1} \\
& \pm \exp \{\frac{ika^2}{2d} \frac{1+M^{-m}}{1-M^{-m}}\} e^{2imkD} M^{m/2} \Gamma_m(-a) q(\frac{M^{-1}-M^{1-m}}{1-M^{-m}} a) \\
& \times (1-M^{-m}) (1 - \frac{aM^{-m}(1+M^{-2})}{(1-M^{-m})(a-x/M)})^{-1}] \\
& + d^{\frac{1}{2}} a\hat{f}(d,a) (1-M^{-2}) \} \quad .
\end{aligned}
\tag{41}
$$

It is necessary now to say more about the functions $\hat{f}$ and $\hat{g}$. If we start with Eq. (25), propagate $\hat{f}$ and $\hat{g}$ to the right end of the cavity using the rate equation (23), and substitute into Eq. (30), we obtain the following functional equation for $\hat{f}(d,x)$:

$$\{(\rho_N-d)^{-\frac{1}{2}} e^{ika^2/2d} [f_N(d,x) \pm f_N(d,-x)] + \hat{f}(d,x)\}$$

$$x \, e^{2ikD} \, M^{-\frac{1}{2}} \, \exp \left\{ \int_d^{Md} G(\rho', Mx) \, d\rho' + \int_d^{Md} G(\rho', x\rho'/d) \, d\rho' \right\} \tag{42}$$

$$= \hat{f}(d, Mx) \quad .$$

From Eq. (35) we see that $s_N(x) \simeq a/M$ for large N. Therefore, from Eqs. (34) and (40) we obtain

$$f_N(d,x) = e^{2i(N-1)kD} \, M^{(N-1)/2} \, [\Gamma_N(x)/\Gamma_1(a/M)] \, f_1(d, a/M)$$

$$\tag{43}$$

$$= e^{2iNkd} \, M^{N/2} \, \Gamma_N(x) \, q(a/M)/[a(1-M^{-2})] \quad .$$

Substituting Eq. (43) into Eq. (42) and using Eqs. (37) and (38) gives for large N

$$\{ d^{-\frac{1}{2}} \, \exp(ika^2/2d) \, \mu^N \, [\Gamma_N'(x) \pm \Gamma_N'(-x)] \, q(a/M) \, a^{-1} \, (1-M^{-2})^{-1} + \hat{f}(d/x) \}$$

$$x \, \mu \, \exp \left\{ \int_d^{Md} G'(\rho', Mx) \, d\rho' + \int_d^{Md} G(\rho', x\rho'/d) \, d\rho' \right\}$$

$$= \hat{f}(d, Mx) \quad . \tag{44}$$

We choose N sufficiently large that $\Gamma_N'(x)$ has reached its limiting form. This may or may not require a larger N than the Horwitz criterion $M^N = 250 \, F_{eff}$, depending on the particular problem being solved. By a consideration of the ray paths for large N, one can see that $\Gamma_N'(x)$ is a symmetric function. The solution of Eq. (44) for the antisymmetric modes is simply $\hat{f} = 0$. The solution of Eq. (44) for the symmetric modes

50

is

$$\hat{f}(d,x) = [\mu^{N+1}/(1-\mu)]\ d^{-\frac{1}{2}}\exp{(ika^2/2d)}\ 2\Gamma_N{}'(x)\ q(a/M)\ a^{-1}\ (1-M^{-2})^{-1}.$$

(45)

This may be verified directly by substituting Eq. (45) into Eq. (44). In deriving Eq. (45) we have taken the limit $N \to \infty$ in certain of the factors (such as the phase). In numerical calculations it is actually simpler not to use the limiting form. Then $\hat{f}(d,x)$ has the same structure as the other terms in Eq. (20) (specialized to $z = D$) except for division by $(1-\mu)$. In the subsequent analysis we do sometimes use the limiting form and sometimes do not, as is convenient.

If we set $x = a$ in Eq. (45) and insert into Eq. (41), we get an equation in which the only unknown amplitude is $q(x)$. However, further approximation is necessary in order to get a tractable polynomial equation for μ. We wish to make an approximation in which $q(x)$ is constant and can be divided out of Eq. (41). There is no unique way to do this. One way is to neglect M^{-m} compared to one everywhere where M^{-m} appears in Eq. (41) except in the phases. A second way is to approximate the angles of all the shadow boundaries by a/d. With either of these approximations it is consistent to regard $q(x)$ as constant. Horwitz uses the second approximation. For the most part, so do we. However, there seems to be no obvious reason why one approximation is better than the other. Fortunately, in those cases in which we have done the calculation both ways, the results are in very good agreement with each other.

Combining Eqs. (41) and (45), dividing by q, using the second approximation just described, and also using Eqs. (37), (38) and (3), we obtained the desired polynomial equation for μ:

51

$$1 = -\frac{1}{2\pi} (i/2F_{eff})^{\frac{1}{2}} \{ \sum_{m=1}^{N+1} [\exp \{2\pi i \; F_{eff} \; \beta_m\} \; \beta_m^{-\frac{1}{2}}$$

$$x \; \Gamma_m'(a) \pm \exp \{2\pi i \; F_{eff}/\beta_m\} \; \beta_m^{\frac{1}{2}} \; \Gamma_m'(-a)] \; \mu^m \tag{46}$$

$$x \; (1/(1-\mu) \text{ for symmetric modes if } m = N+1)\} \quad ,$$

where

$$\beta_m = (1-M^{-m})/(1+M^{-m}) \quad . \tag{47}$$

If we had used the first approximation, the factors $\beta_m^{-\frac{1}{2}}$ and $\beta_m^{\frac{1}{2}}$ would have been absent from Eq. (46). In the case of a bare resonator $[\Gamma_m'(\pm a) = 1]$ Eq. (47) becomes the same as Horwitz's polynomial, aside from differences due to an overall complex conjugation between our theory and Horwitz's theory.

The rays along which the gain is integrated to give $\Gamma_n'(\pm a)$ are rays which leave the mirror edge at point (d,a), make n round trips of the cavity, and end up at point $(d,\pm a)$. Some of the ray paths are shown in Figure 3 for a resonator with $M = 2.5$. Those rays which return to point (d,a) do so by retracing in reverse direction the path which they travel on their first n one-way transits. Because of the assumed symmetry of the gain, the total integrated gain along those ray paths which arrive at $(d,-a)$, as well as those which arrive at (d,a), is just twice the integrated gain along the first n one-way transits. One can see in Figure 15 that the ray paths for large n approximate the ray paths of the geometrical theory.

Once Eq. (46) has been solved for μ, the amplitudes $f_n(d,x)$ and $\hat{f}(d,x)$ are easily solved for. From Eq. (40) we get (putting $q = 1$)

$$f_1(d,x) = \mu M \Gamma_1'(x)/(a-x/M) \quad . \tag{48}$$

52

The amplitude $\hat{f}(d,x)$ is given by Eq. (45) (with q = 1) for the symmetric modes and is zero for the antisymmetric modes.

The total field amplitude f(D,x) of the right-traveling wave on the output-mirror plane is found by using Eqs. (49) and (45) in Eq. (20). However, this does not give a valid solution except well inside the shadow boundaries. In particular, Eq. (48) diverges at x = Ma. In the next section we show how to eliminate this divergence.[8]

2. Extension Through the Shadow Boundaries

So far we have restricted our attention to points well within the shadow boundaries. In order to extend our results to large $|x|$ we need a better approximation to the integral I than that given in Eq. (28). We write I in the form

$$I = \exp[i(C-B^2/A)] \int_{-1}^{1} \exp[iA(\eta-B/A)^2]\, F(\eta)\, d\eta$$

$$\times (A/i\pi)^{\frac{1}{2}} \int_{-\infty}^{\infty} \exp(iA\xi^2)\, d\xi , \qquad (50)$$

where we have simply multiplied by an integral whose value is one. We interpret η and ξ as Cartesian coordinates, so that the integration in Eq. (50) is over an infinite strip. Next we convert to polar coordinates r and ϕ centered at $\xi = 0$, $\eta = B/A$, as illustrated in Figure 16. First suppose that $|B/A| \leq 1$. Then

$$I = (A/i\pi)^{\frac{1}{2}} \exp[i(C-B^2/A)] \{\int_{-\pi/2}^{\pi/2} d\phi \int_{0}^{(1-B/A)\,\sec\phi} F(\eta) r dr \exp(iAr^2)$$

$$+ \int_{\pi/2}^{3\pi/2} d\phi \int_{0}^{(-1-B/A)\,\sec\phi} F(\eta) r dr \exp(iAr^2) \}. \qquad (51)$$

53

We wish to obtain an approximate expression for I which is valid if $F(\eta)$ is slowly varying. We do this by integrating by parts according to

$$r \exp(iAr^2) F(\eta) = \frac{1}{2iA} F(\eta) \frac{\partial}{\partial r} [\exp(iAr^2)]$$

$$= \frac{1}{2iA} \{\frac{\partial}{\partial r} [\exp(iAr^2) F(\eta)] - \exp(iAr^2) \frac{\partial}{\partial r} F(\eta)\} \tag{52}$$

and neglect the term involving the derivative of $F(\eta)$. Then Eq. (51) becomes

$$I \simeq (i\pi/A)^{\frac{1}{2}} \exp[i(C-B^2/A)] f(B/A) - (i/4\pi A)^{\frac{1}{2}}$$

$$\tag{53}$$

$$\times [e^{i(A-2B+C)} F(1) R(A(1-B/A)^2) + e^{i(A+2B+C)} F(-1) R(A(1+B/A)^2)] \quad ,$$

where the function $R(p)$ is defined as

$$R(p) \equiv \int_{-\pi/2}^{\pi/2} \exp(ip \tan^2 \phi)\, d\phi. \tag{54}$$

The function $R(p)$ is essentially the Rubinowicz line integral appropriate to a straight edge.[9] It is possible to derive corrections to Eq. (53) involving the first and higher derivatives of $F(\eta)$ at $\eta = B/A$, 1, and -1. However, we assume that Eq. (53) is an adequate approximation.

If we now consider the case $B/A \geq 1$, we obtain instead of Eq. (53) the expression

$$I \simeq -(i/4\pi A)^{\frac{1}{2}} [-e^{i(A-2B+C)} F(1) R(A(1-B/A)^2)$$

$$\tag{55}$$

$$+ e^{i(A+2B+C)} F(-1) R(A(1+B/A)^2)] \quad .$$

Since $R(0) = \pi$, we see that Eqs. (53) and (55) give the same result when $A = B$. An expression for I which is valid for all values of B/A is given by

$$I \simeq (i\pi/A)^{\frac{1}{2}} \exp[i(C-B^2/A)] \; F(B/A) \; \theta(A^2-B^2) - (i/4\pi A)^{\frac{1}{2}}$$

$$\times [e^{i(A-2B+C)} \; F(1) \; R(A(1-B/A)^2) \; \varepsilon(A-B) \tag{56}$$

$$+ \; e^{i(A+2B+C)} \; F(-1) \; R(A(1+B/A)^2) \; \varepsilon(A+B)] \quad ,$$

where

$$\theta(p) \equiv \begin{cases} 1, \; p > 0 \; , \\ 0, \; p < 0 \; , \end{cases} \tag{57}$$

$$\varepsilon(p) \equiv \begin{cases} 1, \; p > 0 \; , \\ -1, \; p < 0 \; . \end{cases} \tag{58}$$

Equation (53) can be reduced to Eq. (28) by making a stationary phase approximation of Eq. (54) valid for large p:

$$R(p) \simeq (i\pi/p)^{\frac{1}{2}} \; . \tag{59}$$

The physical meaning of Eq. (56) is that diffraction of a cylindrical wave by a slit gives rise to a total field that is the sum of three contributions: the undiffracted field, chopped off at the geometrical shadow boundaries, and two cylindrical waves emanating from the edges of the slit. These latter waves are not quite proper cylindrical waves, however, since they behave peculiarly near the shadow boundaries. In fact, they

55

are discontinuous at the shadow boundaries in just such a way that the total field is continuous. The right-traveling field in the resonator may be viewed as a set of cylindrical waves emanating from the points $(\rho_n, \pm x_n)$ $n = 2, \ldots, N$ and a plane wave. These waves are diffracted by a virtual aperture at $(\rho_1, \pm x_1)$. Similarly, the left-traveling field may be viewed as a set of cylindrical waves emanating from the points $(\rho_n, \pm x_n)$, $n = -1, \ldots, -N+1$, and $(0,0)$. These waves are diffracted at the output mirror $(\rho_0, \pm x_0)$. In accordance with Eq. (56) the amplitudes $f_2, \ldots, f_N$ and $\hat{f}$ at $\rho = d$ are to be chopped off at the shadow boundaries. The shadow boundaries of the plane wave are at $x = \pm Ma$. The shadow boundaries of the cylindrical waves are at $x = Ma(1 + M^{-n-1})/(1 + M^{-n+1})$ and $x = -Ma(1 - M^{-n-1})/(1 - M^{-n+1})$. These differ significantly from $x = \pm Ma$ if n is small. Equation (49) is altered to read

$$f_n(d,x) = \mu^n M^n \Gamma_n'(x) (a - s_n(x)/M)^{-1} \theta(Ma(1+M^{-n-1})/(1+M^{-n+1}) - x)$$

$$(60)$$

$$x\ \theta(x + Ma(1-M^{-n-1})/(1-M^{-n+1}))\ ,\quad n = 2, \ldots, N\ .$$

Equation (45) is modified similarly by multiplying by $\theta(Ma-x)\ \theta(x+Ma)$. We see that Eq. (60) is well-behaved and that $f_n(d,x)$ is, in fact, slowly varying. The singularity where $s_n(x) = Ma$ occurs at $x = M^n a$, which is well outside the shadow boundaries, provided that M is not close to one.

It remains now to determine $f_1(d,x)$. To this end we calculate the edge-diffraction contributions to Eq. (27), using Eqs. (56) and (20). We find that

$$g_0(\rho,x) = -\frac{1}{2\pi} d^{\frac{1}{2}} e^{2ikD} \{ \sum_{n=1}^{N-1} (\rho-d)^{\frac{1}{2}} \rho_n^{-\frac{1}{2}} (\rho-\rho_{-n})^{-\frac{1}{2}}$$

$$\times [\exp\{\frac{ik}{2}(x_n-a)^2/(\rho_n-d)\} f_n(d,a) R(\frac{kd}{2}(\alpha_n^{(+)}-\alpha)^2$$

$$\times (\rho-d)(\rho_n-d)(\rho-\rho_{-n})^{-1} \rho_n^{-1}) \, \varepsilon(\alpha_n^{(+)}-\alpha) \tag{61}$$

$$\pm \exp'\{\frac{ik}{2}\frac{(a+x_n)^2}{\rho_n-d}\} f_n(d,-a) R(\frac{kd}{2}(\alpha_n^{(-)}-\alpha)^2 (\rho-d)(\rho_n-d)(\rho-\rho_{-n})^{-1} \rho_n^{-1})$$

$$\times \varepsilon(\alpha_n^{(-)}-\alpha)] + (\rho-d)^{\frac{1}{2}} \rho^{-\frac{1}{2}} [e^{ika^2/2d} \rho_N^{-\frac{1}{2}} (f_N(d,a) \pm f_n(d,-a))$$

$$+ \hat{f}(d,a)] R(\frac{kd}{2}(\frac{a}{d}-\alpha)^2 (\rho-d) \rho^{-1}) \, \varepsilon(\frac{a}{d}-\alpha)\}$$

$$\times \exp'\{\int_d^\rho G(\rho', a+(\rho'-d)\alpha) \, d\rho'\} \quad .$$

Equation (61) reduces to Eq. (31) well inside the shadow boundaries, where Eq. (59) is valid, except that, to be consistent with our truncation scheme, we extend the summation in Eq. (61) only up to $n = N-1$ and lump the term for which $n = N$ together with the term containing $\hat{f}(d,a)$. To calculate $f_1(\rho,x)$ we regard the points $(\rho_1,\pm x_1)$ as edges of a virtual aperture illuminated by cylindrical waves emanating from points $(\rho_n,\pm x_n)$, $n = 2,\ldots,N$ and by a plane wave. Near $\rho = \rho_1$ the total amplitude $f(z,x)$ is given by the integral

$$f(Md-\rho,x) = \frac{1}{2\pi} [-2\pi ki/(\rho_1-\rho)]^{\frac{1}{2}} \int_{-x_1}^{x_1} dx' \, f(Md-\rho_1,x')$$

$$\times \exp[\frac{ik}{2}(x-x')^2/(\rho_1-\rho)] \quad . \tag{62}$$

57

If we let $\eta = x'/x_1$ and use the form of $f(Md-\rho_1, x_1\eta)$ implied by Eq. (20) then we can use Eq. (56) to carry out the integration over η. The function $f_1(\rho, x)$ comes from the second term in Eq. (56), which describes edge diffraction at $\eta = 1$. We obtain

$$f_1(\rho, x) = -\frac{1}{2\pi} \left\{ \sum_{n=2}^{N} (\rho_1-\rho)^{\frac{1}{2}} (\rho_n-\rho)^{-\frac{1}{2}} \left[\exp\left\{ i\frac{k}{2} \frac{(x_1-x_n)^2}{\rho_n-\rho_1} \right\} \right. \right.$$

$$\times f_n(\rho_1, x_1) \, R\left(\frac{k}{2} (\rho_1-\rho)(\rho_n-\rho_1)(\rho_n-\rho)^{-1} \left(\frac{x_1-x}{\rho_1-\rho} + \frac{x_1-x_n}{\rho_n-\rho_1}\right)^2\right)$$

$$\times \varepsilon\left(\frac{x_1-x}{\rho_1-\rho} + \frac{x_1-x_n}{\rho_n-\rho_1}\right) \pm \exp\left\{ i\frac{k}{2} \frac{(x_n+x_1)^2}{\rho_n-\rho_1} \right\} f_n(\rho_1, -x_1) \quad (63)$$

$$\times R\left(\frac{k}{2} (\rho_1-\rho)(\rho_n-\rho_1)(\rho_n-\rho)^{-1} \left(\frac{x_1-x}{\rho_1-\rho} + \frac{x_1+x_n}{\rho_n-\rho_1}\right)^2\right) \varepsilon\left(\frac{x_1-x}{\rho_1-\rho} + \frac{x_1+x_n}{\rho_n-\rho_1}\right)\right]$$

$$\left. + (\rho_1-\rho)^{\frac{1}{2}} \hat{f}(\rho_1, x_1) \, R\left(\frac{k}{2} (\rho_1-\rho) \left(\frac{x_1-x}{\rho_1-\rho}\right)^2\right) \varepsilon(x_1-x) \right\} \quad .$$

If ρ is not close to ρ_1, then Eq. (63) must be modified by multiplying the right-hand side by the exponential of the gain integrated along the rays emanating from (ρ_1, x_1). In particular, at $\rho = Md$ one must multiply by

$$\exp\left\{ \int_d^{Md} G\left(\rho', \; a+(\rho'-d) \frac{x-a}{d(M-1)}\right) d\rho' \right\}$$

in order to match $f_1(Md, x)$ to $g_0(Md, x)$ on the concave mirror:

$$(\rho_1-Md)^{-\frac{1}{2}} f_1(Md, x) = (Md-d)^{-\frac{1}{2}} g_0(Md, x) \quad . \quad (64)$$

58

At $\rho = d$ the right hand side of Eq. (63) is to be multiplied by $\Gamma_1(x)$. The coefficients $f_n(\rho_1, \pm x_1)$ and $\hat{f}(\rho_1, x_1)$ appearing in Eq. (63) are found by substituting Eqs. (63) and (61) into Eq. (64). One gets

$$f_n(\rho_1, \pm x_1) = e^{2ikD} M^{\frac{1}{2}} f_{n-1}(d, \pm a) , \qquad n = 2, \ldots, N , \tag{65}$$

$$\hat{f}(\rho_1, x_1) = e^{2ikD} M^{-\frac{1}{2}} [e^{ika^2/2d} \rho_N^{-\frac{1}{2}} (f_N(d,a) \pm f_N(d,-a)) + \hat{f}(d,a)] . \tag{66}$$

The values of $f_n(d, \pm a)$ and $\hat{f}(d,a)$ are gotten by setting $x = \pm a$ in Eqs. (49) and (45):

$$f_n(d, \pm a) = \mu^n M^n \Gamma_n'(\pm a) (1 \pm M^{-n})/[a(1-M^{-2})] , \tag{67}$$

$$\hat{f}(d,a) = d^{-\frac{1}{2}} a^{-1} (1-M^{-2})^{-1} \exp(ika^2/2d) (1 \pm 1) \Gamma_N'(a) \mu^{N+1}/(1-\mu). \tag{68}$$

If we use Eq. (67) (for $n = N$) and Eq. (68) in Eq. (66) and use the limiting form of f_N for large N, we get

$$\hat{f}(\rho_1, x_1) = e^{2ikD} M^{-\frac{1}{2}} \exp(ika^2/2d) d^{-\frac{1}{2}} a^{-1} (1-M^{-2})^{-1} \tag{69}$$

$$\times (1 \pm 1) \Gamma_N'(a) \mu^N/(1-\mu).$$

Substituting Eq. (67) into Eq. (65) gives

$$f_n(\rho_1, \pm x_1) = e^{2ikD} M^{\frac{1}{2}} \mu^{n-1} M^{n-1} \Gamma_{n-1}'(\pm a) (1 \pm M^{-n+1})/[a(1-M^{-2})] . \tag{70}$$

59

Next we substitute Eqs. (69) and (70) into Eq. (63), set $\rho = d$, and multiply the right-hand side of Eq. (63) by $\Gamma_1(x)$. This gives

$$
f_1(d,x) = -\frac{1}{2\pi} \Gamma_1'(x) \, M(1-M^{-2})^{-\frac{1}{2}} \, a^{-1} \sum_{n=2}^{N+1} (M^{2n}-1)^{-\frac{1}{2}}
$$

$$
\times \, \mu^n M^n \left[\exp'\left\{ i2\pi F_{eff} \frac{1-M^{-n+1}}{1+M^{-n+1}} \right\} \Gamma_{n-1}'(a) \, (1+M^{-n+1}) \right.
$$

$$
\times \, R\!\left(2\pi F_{eff} \frac{M^{-2}-M^{-2n}}{(1-M^{-2n})(1-M^{-2})} \; \left(M\frac{1+M^{-1-n}}{1+M^{-n+1}} - \frac{x}{a}\right)^2 \right)
$$

(71)

$$
\times \, \varepsilon\!\left(M\frac{1+M^{-n-1}}{1+M^{-n+1}} - \frac{x}{a}\right) \pm \exp'\left\{ i2\pi F_{eff} \frac{1+M^{-n+1}}{1-M^{-n+1}} \right\} \Gamma_{n-1}'(-a)
$$

$$
\times \, (1-M^{-n+1}) \, R\!\left(2\pi F_{eff} \frac{M^{-2}-M^{-2n}}{(1-M^{-2n})(1-M^{-2})} \; \left(M\frac{1-M^{-n-1}}{1-M^{-n+1}} - \frac{x}{a}\right)^2 \right)
$$

$$
\times \, \varepsilon'\!\left(M\frac{1-M^{-n-1}}{1-M^{-n+1}} - \frac{x}{a}\right) \bigg] \times (1/(1-\mu) \text{ for symmetric modes if } n = N+1).
$$

The total amplitude $f(D,x)$ is found by setting $z = D$ in Eq. (20) and substituting Eqs. (60), (45) multiplied by θ functions, and (71) into Eq. (20). After some algebraic simplification using Eq. (35) and assuming $x \geq 0$ we obtain the basic result:

$$
f(D,x) = \sum_{n=2}^{N+1} \left\{ \mu^n (1-M^{-2n})^{\frac{1}{2}} (1-M^{-2})^{-1} \left[\exp'\left\{ i2\pi F_{eff} \frac{(1-M^{-n}x)^2}{1-M^{-2n}} \right\} \Gamma_n'(x) \right. \right.
$$

$$
\times \, (1-M^{-n}x)^{-1} \, \theta\!\left(\frac{1+M^{-n-1}}{1+M^{-n+1}} - \frac{x}{M}\right) \pm \exp\left\{ i2\pi F_{eff} \frac{(1+M^{-n}x)^2}{1-M^{-2n}} \right\} \Gamma_n'(-x)
$$

$$x \ (1+M^{-n}x)^{-1} \ \theta \left(\frac{1-M^{-n-1}}{1-M^{-n+1}} - \frac{x}{M} \right)]$$

$$- \ [(\exp \ \{i2\pi \ F_{eff} \ \frac{(1-M^{-1}x)^2}{1-M^{-2}}\} \ \frac{1}{2\pi} \ \Gamma_1{}'(x) \ (1-M^{-2})^{-1}\{\mu^n(1-M^{-2n})^{-\frac{3}{2}}$$

$$x \ [\exp \ \{i2\pi \ F_{eff} \ \frac{1-M^{-n+1}}{1+M^{-n+1}}\} \ \Gamma_{n-1}'(1) \ \ (1+M^{-n+1}) \tag{72}$$

$$x \ R(2\pi \ F_{eff} \ \frac{1-M^{-2n+2}}{(1-M^{-2n})(1-M^{-2})} \ \left[\frac{1+M^{-1-n}}{1+M^{-n+1}} - \frac{x}{M} \right]^2) \ \epsilon \left(\frac{1+M^{-n-1}}{1+M^{-n+1}} - \frac{x}{M} \right)$$

$$\pm \ \exp \ \{i2\pi \ F_{eff} \ \frac{1+M^{-n+1}}{1-M^{-n+1}}\} \ \Gamma_{n-1}'(-1) \ (1-M^{-n+1})$$

$$x \ R(2\pi \ F_{eff} \ \frac{1-M^{-2n+2}}{(1-M^{-2n})(1-M^{-2})} \ \left[\frac{1-M^{-n-1}}{1-M^{-n+1}} - \frac{x}{M} \right]^2) \ \epsilon \left(\frac{1-M^{-n-1}}{1-M^{-n+1}} - \frac{x}{M} \right)]\})$$

$$\pm \ \text{(same expression with x replaced by -x)]} \} \ x \ (1/(1-\mu) \ \text{for}$$

the symmetric modes if n = N + 1)   .

In Eq. (72) we have set a = 1, i.e., x is measured in units of a. It is straightforward to check that Eq. (72) is continuous at the shadow boundaries. However, this does not rule out the possibility of significant discontinuities in slope. It is possible that such discontinuities occur at values of M very close to one. In the numerical calculations which we have carried out, where we take M = 2.0 or M = 2.9, there is no noticeable lack of smoothness in f(D,x).

For the symmetric modes the coefficients of μ^n in Eq. (72) become independent of n for n sufficiently large. Note that the last term

(for n = N + 1) is to be divided by 1-μ. The exact value of N is unimportant, so long as it is sufficiently large. Further increases in N simply add more high-loss unphysical modes by increasing the degree of the polynomial in Eq. (46). For the lowest-loss mode μ is typically quite close to one, especially near half-integral values of F_{eff}, so that the term which has (1-μ) as a divisor is considerably larger than the other terms.

For the antisymmetric modes the coefficients of μ^n in Eq. (72) approach zero as n becomes large. Physically this means that waves emanating from the two mirror edges bounce back and forth and spread out until they cancel each other by destructive interference.

3. Numerical Calculation of the Symmetric Modes

In this section we present a variety of solutions for symmetric modes of strip confocal unstable resonators. Since the lowest loss mode is generally symmetric, the antisymmetric modes are of less interest, and we do not discuss them further here.

We present solutions both for bare resonators and for loaded resonators. In the case of loaded resonators, we assume that the gain G is independent of ρ, extends the entire length of the cavity, and depends on x according to

$$G'(x) = A [\exp(-\beta x^2)-1]. \tag{73}$$

We take $\beta = 1.5/a^2$ and take

$$A = 1/4 \ln M/[(M-1)d] \tag{74}$$

or

$$A = -1/8 \ln M/[(M-1)d] . \tag{75}$$

In the first case we have a Gaussian gain distribution. The value of A is chosen such that for the lowest-loss mode, for which $|\mu| \approx 1$, the gain

$$G(x) = G'(x) + 1/4 \ln |M\mu|/[(M-1)d] \tag{76}$$

falls to near zero for large x.

In the second case we have a negative Gaussian gain distribution. In this case the gain $G(x)$ for the lowest-loss mode dips to about 2/3 of its large-x value as $x \to 0$.

We do not claim that either of these forms for G' is realistic. Finding a realistic form for G would require an iterative calculation. Such an iterative calculation would be worthwhile for a three-dimensional resonator with a rectangular-edged output mirror, but is probably not worthwhile for a strip resonator. The main point of the present work is to test the general soundness of our theoretical approach in a simple, two-dimensional geometry. Once this has been tested, it appears straightforward to proceed to three dimensions.

We have developed two codes, called ROOTS and MODES, which have been used to calculate the results presented here. ROOTS uses the sub-routine CPQR (provided by Kirtland AFB) to calculate the roots μ of the complex polynomial in Eq. (46). For the examples presented the degree of the polynomial which we use ranges between 9 and 13. In the case of a loaded resonator it is necessary to calculate $\Gamma_n'(\pm a)$. This is done by straightforward numerical integration of Eq. (36). We do this by using parabolic interpolation and Simpson's rule integration. We specify G'(x) on a 25 x 25 grid extending the whole length of the resonator and from x = 0 to x = 4.8a. We have also tried using a 49 x 49 grid

and get essentially the same results. ROOTS does not operate at maximum efficiency, since after each increment in F_{eff}, CPQR starts from scratch and recalculates all of the roots. Horwitz's technique of using previously calculated roots as trial solutions and omitting calculation of roots corresponding to high-loss modes would make ROOTS operate much more efficiently. At present, using a CDC 6400 computer, a calculation of roots at 30 values of F_{eff} typically requires about 7.9 sec execution time for a bare resonator and 14.6 sec for a loaded resonator. Part of the reason for the longer time required for a loaded resonator is that, for most of the cases we have considered, a higher degree of polynomial is required for a loaded resonator in order to make the Γ's converge.

MODES calculates and plots the intensities and phases of the resonator modes. For an M = 2.9 resonator, for example, this involves calculation at 401 values of x/a using a step size of 0.01. This takes about 10.3 sec for a bare resonator. For a loaded resonator one must also calculate $\Gamma_n'(x)$. Since the Γ's are slowly varying, we calculate them using a step size of 0.2 and interpolate onto the finer grid. It is inefficient to calculate the Γ's using Eq. (36). Instead, we calculate them successively using the equation

$$
\Gamma_n'(x) = \exp' \left\{ \int_d^{Md} G'(\rho', \frac{M^{1-n}}{1-M^{-2n}} (-M^{-n}x + a) \right.
$$

$$
+ \frac{\rho'}{d} \frac{M^{-1}}{1-M^{-2n}} (x-M^{-n}a)) \, d\rho' + \int_d^{Md} G(\rho', \frac{1}{1-M^{-2n}}
$$

$$
\times (x-M^{-n}a) + \frac{\rho'}{d} \frac{M^{-n}}{1-M^{-2n}} (-M^{-n}x + a)) \, d\rho' \right\}
$$

$$
\times \Gamma_{n-1}'(\frac{1}{1-M^{-2n}} [(-M^{1-2n} + M^{-1})x + (M^{1-n} - M^{-n-1})a]) \quad .
$$

(77)

64

The time needed to calculate the Γ's is about 5.9 seconds. Since the Γ's do not depend on F_{eff} or on the particular mode being calculated, it is often useful to calculate several different intensity and phase curves in one run while calculating the Γ's only once. The functions $\Gamma_n'(x)$ are shown graphically in Figure for the case of a Gaussian gain distribution in a resonator with $M = 2.9$. For small n the functions are asymmetric, but they approach a symmetric limit function as n becomes large.

The function $R(p)$ which is defined in Eq. (54) must be calculated in order to determine $f(D,x)$ according to Eq. (72). This function may be expressed in terms of the Fresnel integrals $f(x)$ and $g(x)$ by

$$R(p) = \pi(1-i) \{g[(2p/\pi)^{\frac{1}{2}}] + if[(2p/\pi)^{\frac{1}{2}}]. \tag{78}$$

The functions f and g are well behaved and may be conveniently evaluated by means of a rational approximation given in the mathematical literature.[10]

The results presented here are of high quality in the sense that the grids used are sufficiently fine to give results of good accuracy and high resolution. The amount of computation time required is nevertheless not large. If coarser grids were used, the time required would be even smaller.

In Figures 18 and 19 we show plots of $|\lambda|$ versus F_{eff}, where $|\lambda| \equiv 1/|\mu|$. The results are shown in this form to facilitate comparison with Horwitz's results. Figure 18 is for a resonator with $M = 2.9$ and $15.1 \leq F_{eff} \leq 11.0$. Figure 19a is for a bare resonator, Figure 19b is for a resonator containing Gaussian gain distribution, and Figure 19c is for a resonator containing a negative Gaussian gain distribution. Note that the presence of a Gaussian gain distribution enhances the separation of the lowest-loss mode from the other modes, while a negative Gaussian gain distribution has the opposite effect.

65

Figures 20 through 22 show intensity and phase distributions $|f(D,X)|^2$ and arg[f(D,x)] in the output-mirror plane for a resonator with M = 2.9 and F_{eff} = 16.4. The tick marks on the positive side of the horizontal axis indicate the positions of the shadow boundaries. Figure 20 shows the lowest-loss mode of a bare resonator. Figure 21 shows the next-to-lowest-loss eymmetric mode of a bare resonator. The intensities in these two figures are in complete agreement with Horwitz's Figure 24 in the range 0 ≤ x ≤ a where comparison is possible. Note the large peak in intensity in Figure 21 near the shadow boundaries the small intensity near the axis. Also note that while the phase in Figure 20 is nearly constant out to the shadow boundaries, the phase in Figure 21 fluctuates considerably. The apparent (but unreal) discontinuities in phase are merely the result of requiring the phase to lie between -180° and +180°, normalized with respect to the phase at the center of the mirror. Intensities are normalized so that the largest intensity in the range 0 ≤ x ≤ a is unity.

Figure 22 is for the lowest-loss mode of a resonator containing a Gaussian gain distribution. This may well be the first calculation yet performed for a resonator containing distributed gain and having this high a Fresnel number. As one might expect with this sort of gain distribution, the intensity dies off as x increases well before x gets near the shadow boundaries. However, the fine structures of the intensity distributions in Figures 20 and 22 are quite similar. The phase distributions in Figures 20 and 22 are also nearly the same.

Figures 23 through 25 show intensity and phase distributions for a resonator with M = 2.0 and F_{eff} = 8.4. These figures are respectively for the lowest-loss modes of a bare resonator, a resonator with a Gaussian gain distribution, and a resonator with a negative Gaussian gain distribution. These results are for a value of F_{eff} where FFT calculations are feasible, and it would be of considerable interest to have results of FFT calculations to compare with our results.

66

Unfortunately, we have not found anything comparable in the published literature.

We have carried out a number of other mode calculations which space does not permit us to present here. These calculations show no obvious breakdown of the theory at small F_{eff}. Our calculations have used values as low as $F_{eff} = 2.9$. Horwitz claims good agreement with other methods of calculation down to $F_{eff} \simeq 1$. None of these results of other workers extend to the domain $x > a$ or to loaded resonators. We have not tried values of M smaller than 2.0. Our theory breaks down for M too close to one, at least as a practical matter, since the degree of the polynomial required approaches infinity as $M \to 1$. However, it should be possible to get quite a bit closer to M = 1 before this limitation on the theory becomes important.

An extension of the present theory to three-dimensional resonators with rectangular mirrors appears straightforward. Guided by the fact that the paraxial wave equation for a bare resonator can be factored, we propose replacing Eqs. (20) and (21) by equations containing double sums, one sum for each transverse dimension. The waves associated with the terms in these double sums would not simply be cylindrical waves, but would be waves having one caustic on an edge of the output mirror or one of its images and another caustic on an orthogonal edge of a different image. The diagonal terms would correspond to spherical waves emanating from the corners of the mirror images.

It is not clear whether an analogous theory can be developed for resonators with round mirrors. The main difficulty with round mirrors is that the edge-diffraction wave adds constructively to give a caustic on the resonator axis. The behavior at large F_{eff} of resonators with round mirrors is not well understood, since it has not been feasible to carry out mode calculations for these resonators. No evidence of the separation of the lowest-loss mode from the other modes has been found, but it is not known whether interleaving of the low-loss modes

67

persists to very large F_{eff}. We are even further from understanding how the spatial distribution of gain affects the mode behavior.

4. Acknowledgements

REFERENCES

1. A. E. Siegman, "Unstable optical resonators," Appl. Opt. 13, 353-367 (1974). This article gives an extensive review of work on unstable resonators prior to 1974.

2. G. T. Moore and R. J. McCarthy, "Lasers with unstable resonators in the geometrical optics limit," J. Opt. Soc. Am. __, (1976) preceding article.

3. E. A. Sziklas and A. E. Siegman, "Mode calculations in unstable resonators with flowing saturable gain. 2: Fast Fourier transform method," Appl. Opt. 14, 1874-1889 (1975).

4. D. B. Rensch and A. N. Chester, "Iterative diffraction calculations of transverse mode distributions in confocal unstable laser resonators," Appl. Opt. 12, 997-1010 (1973).

5. R. L. Sanderson and W. Streifer, "Unstable laser resonator modes," Appl. Opt. 8, 2129-2136 (1969).

6. P. Horwitz, "Asymtotic theory of unstable resonator modes," J. Opt. Soc. Am. 63, 1528-1543 (1973).

7. A. E. Siegman, "Unstable optical resonators for laser applications," Proc. IEEE 53, 277-287 (1965).

8. P. Horwitz, "Modes in misaligned unstable resonators," Appl. Opt. 15, 167 (1976). This paper of Horwitz's, of which we were unaware until after completion of the work reported here, treats the problem of the shadow boundaries by a different approach than ours, but with equivalent results.

9. M. Born and E. Wolf, <u>Principles of Optics</u> (Pergamon, New York, 1964),
    2nd ed., p. 449. This text also gives references to the original litera-
    ture on the boundary diffraction wave.

10. M. Abramowitz and J. A. Stegun, <u>Handbook of Mathematical Functions</u>
    (Dover, New York, 1965), p. 302.
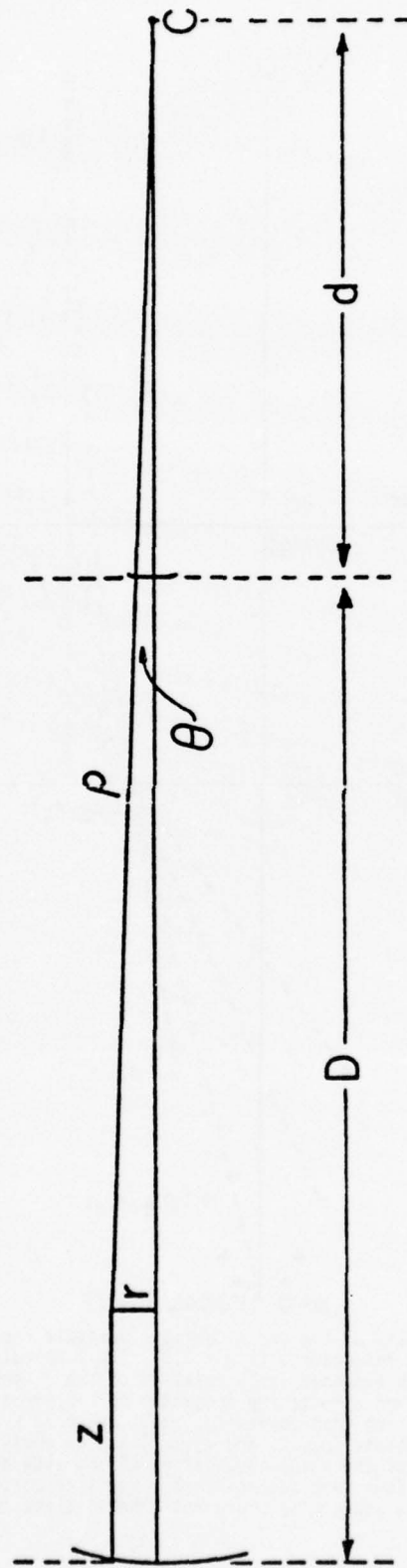
Fig. 13. Geometry of the confocal unstable resonator
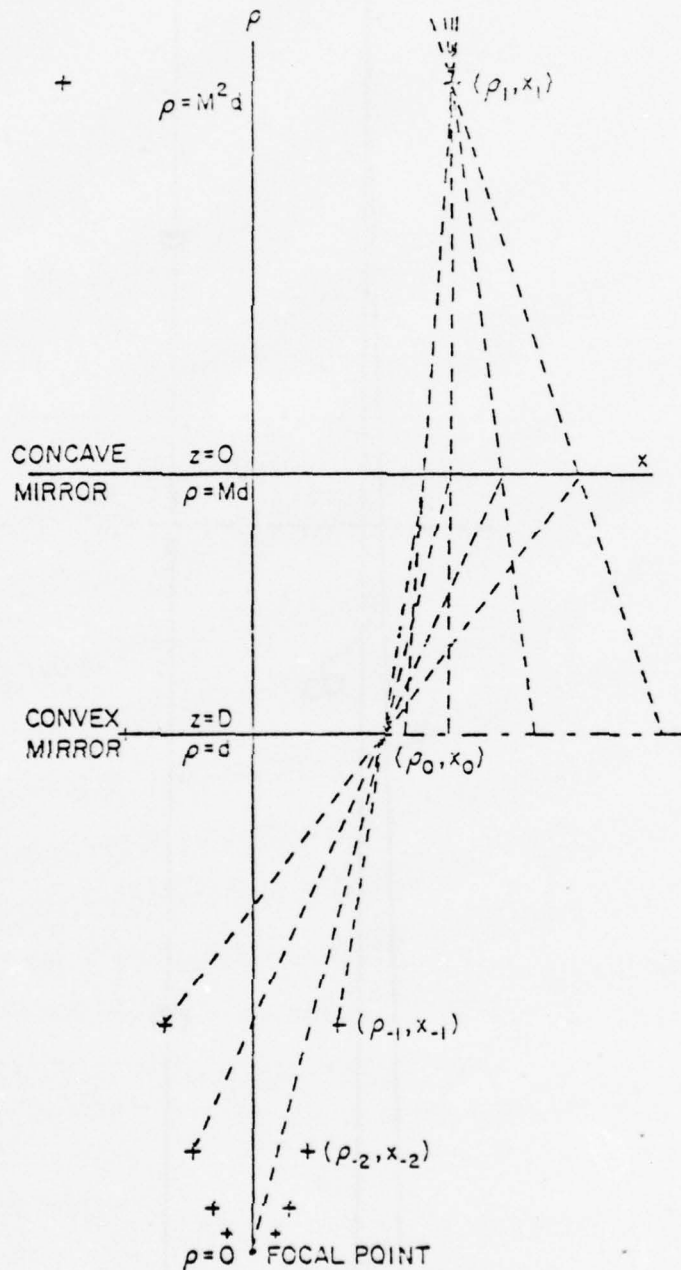
Fig. 14. Geometry of the strip confocal unstable resonator is illustrated
for a resonator with M = 1.5. The x coordinate is shown on
a much expanded scale relative to the ρ coordinate. Edge dif-
fraction effects are accounted for in terms of cylindrical waves
emanating from points (ρ_n, x_n), where $\rho_n = dM^{2n}$ and $x_n = aM^n$.
The points (ρ_0, x_0) and (ρ_1, x_1) act as edges of apertures.
Some of the shadow boundaries on one side of the resonator
are shown iwth dotted lines. For a resonator with large M, the
shadow boundaries would not come so close to the mirror edges.
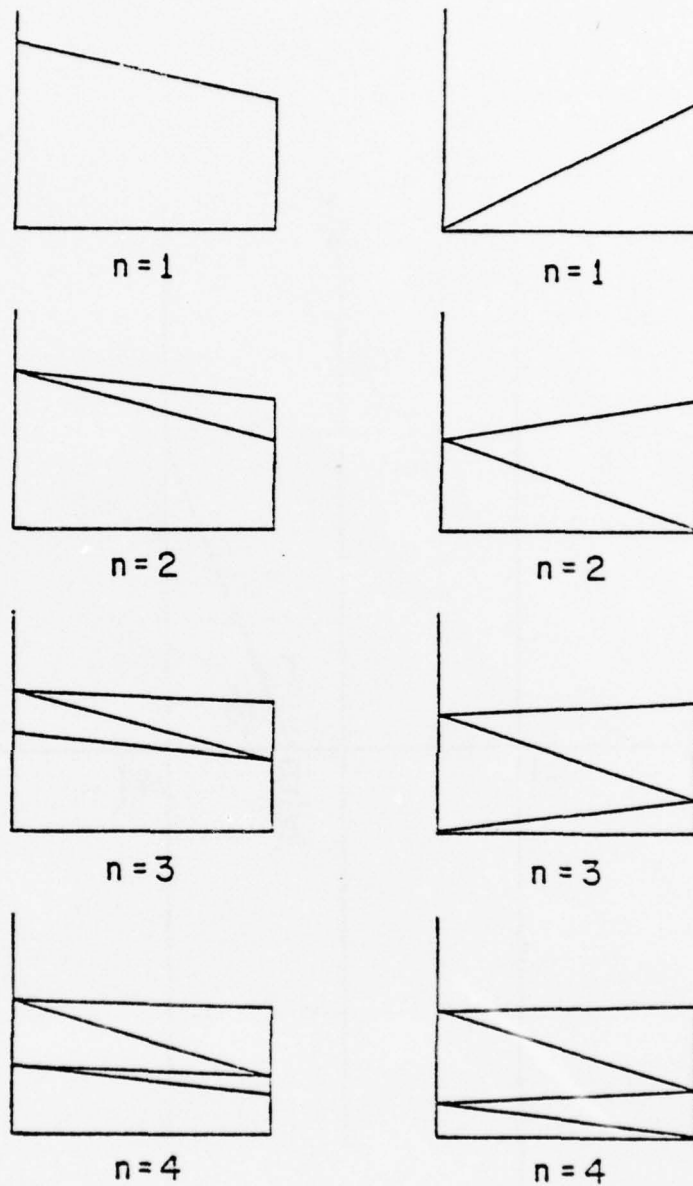
Fig. 15. Ray paths along which the gain is integrated to give $\Gamma_n(\pm a)$ are shown for n = 1,2,3,4. The output mirror edge is in the upper right corner of each diagram and the resonator axis is along the bottom. Rays below the axis (not shown) are the mirror images of those above. Those rays which return to x = a do so by reversing the path by which they zig-zag toward the axis. The diagrams are shown for a resonator with M = 2.5.

73
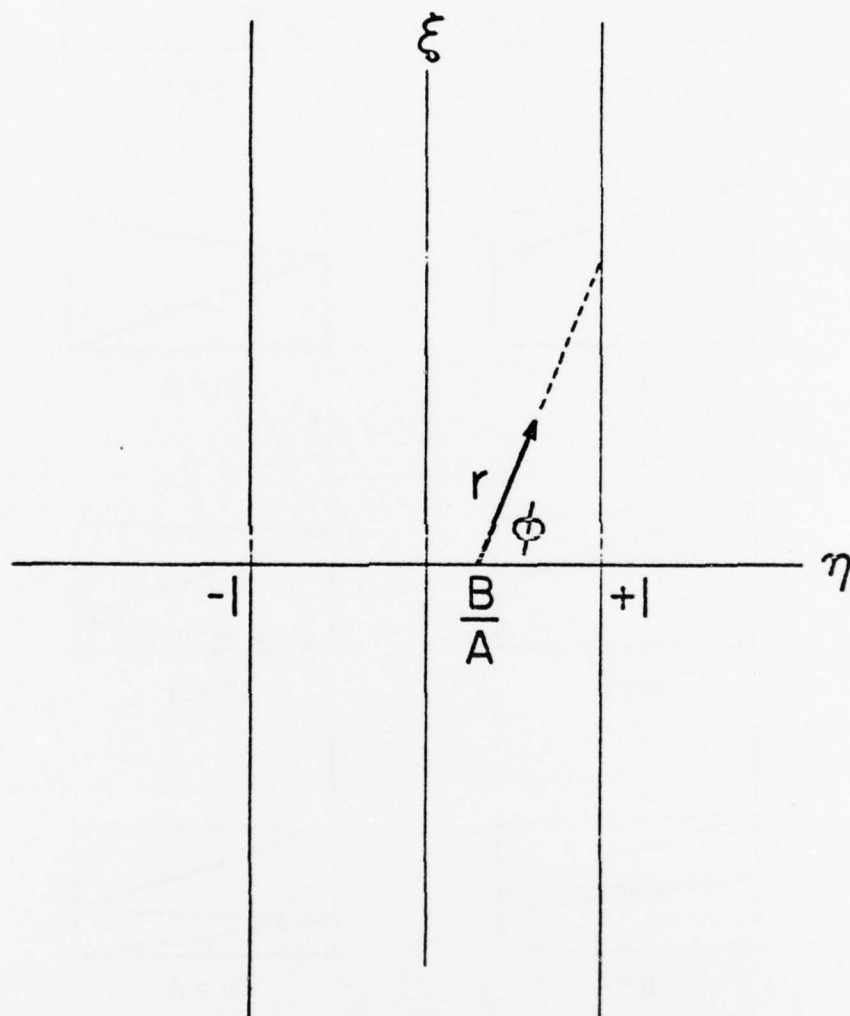
Fig. 16. Coordinate systems used to evaluate the integral I in Eq. (50)
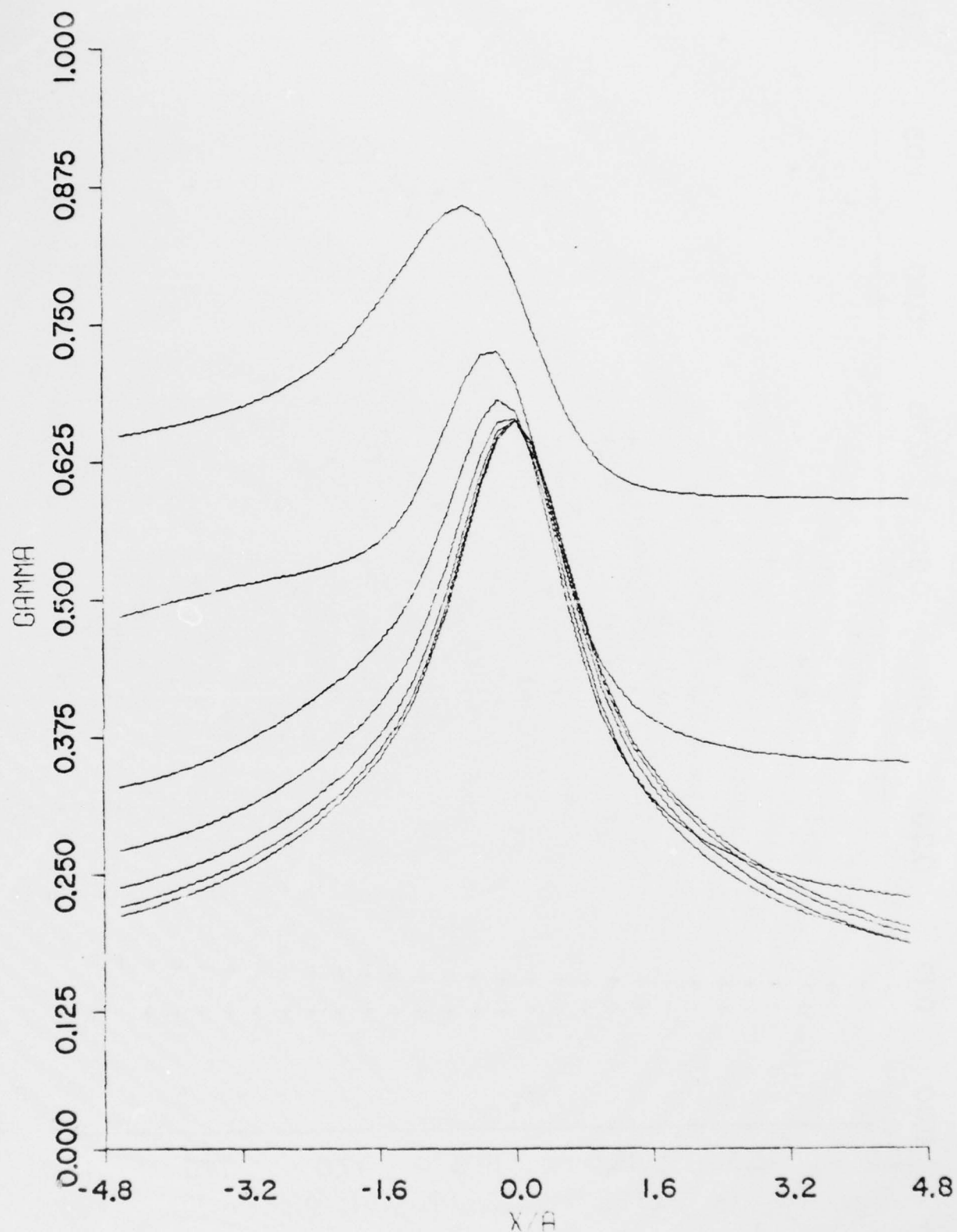
Fig. 17. The functions $\Gamma_n{}'(x)$ for n = 1 through 7 are shown for a resonator with M = 2.9 containing a Gaussian gain distribution. The upper curve is for n = 1. As n increases $\Gamma_n{}'(x)$ approaches a symmetric limit function.

75
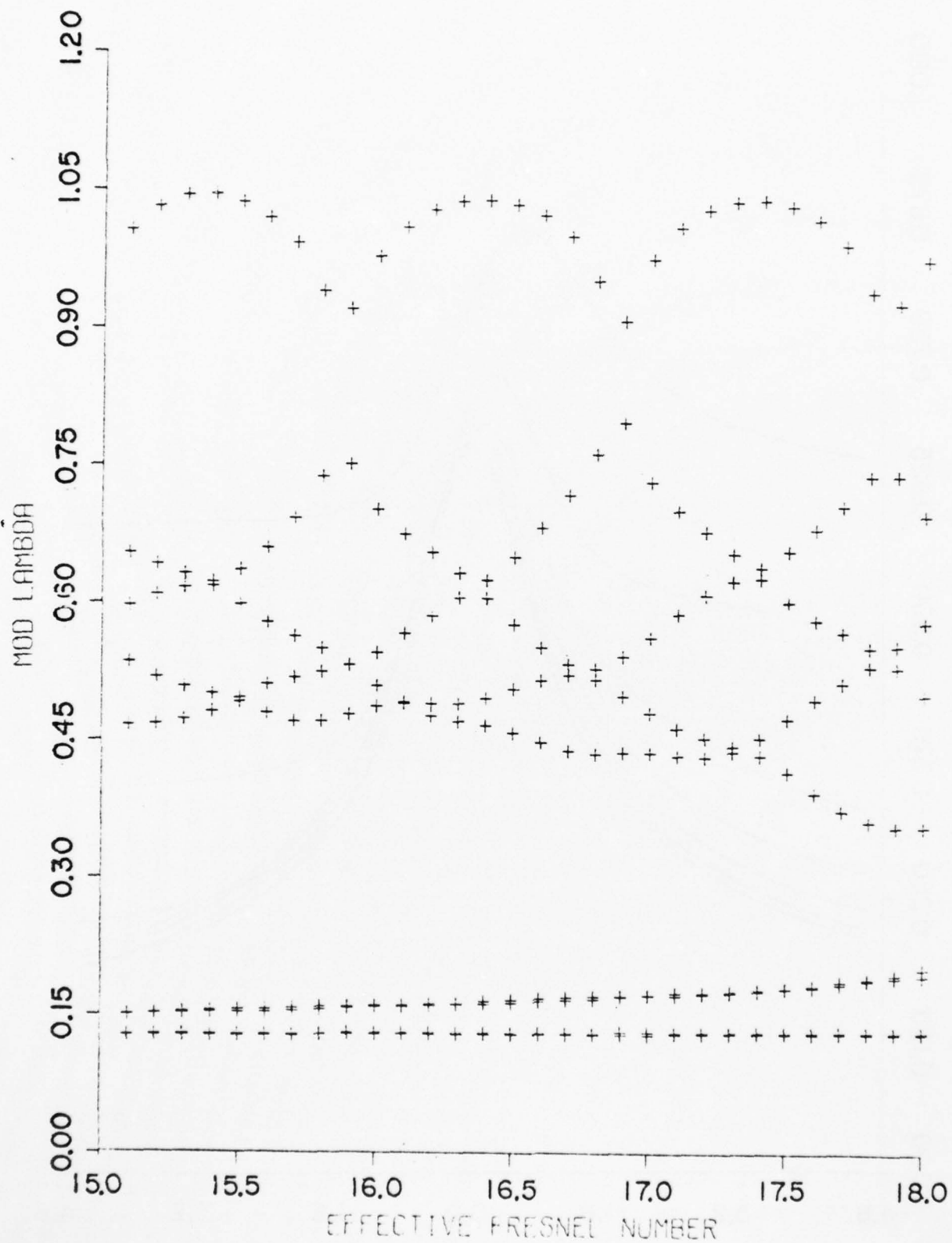
Fig. 18.a. Modulus of λ vs. effective Fresnel number for
M = 2.9, symmetric roots. Bare resonator

76
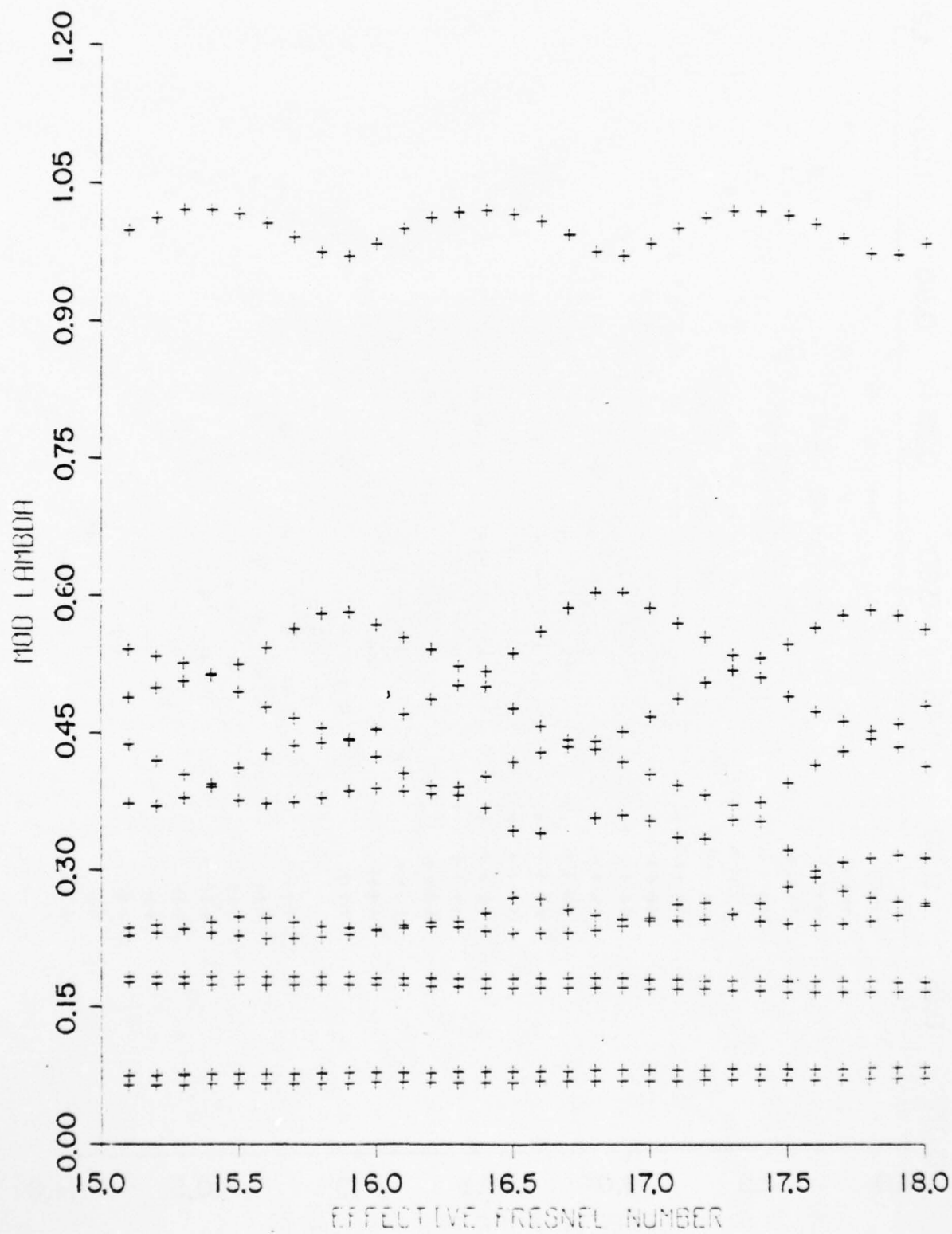
Fig. 18.b. Modulus of λ vs. effective Fresnel number for M = 2.9, symmetric roots. Resonator containing Gaussian gain distribution
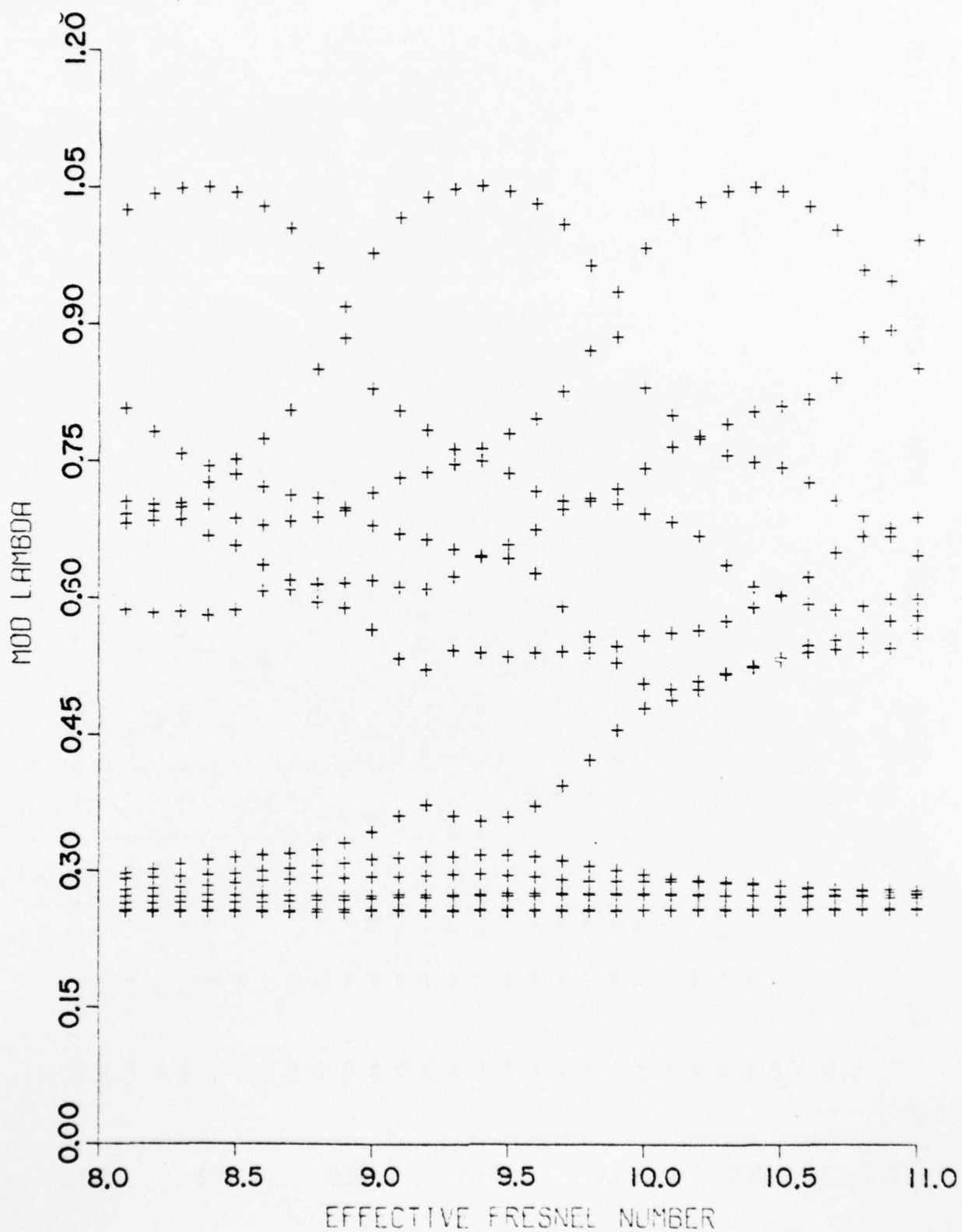
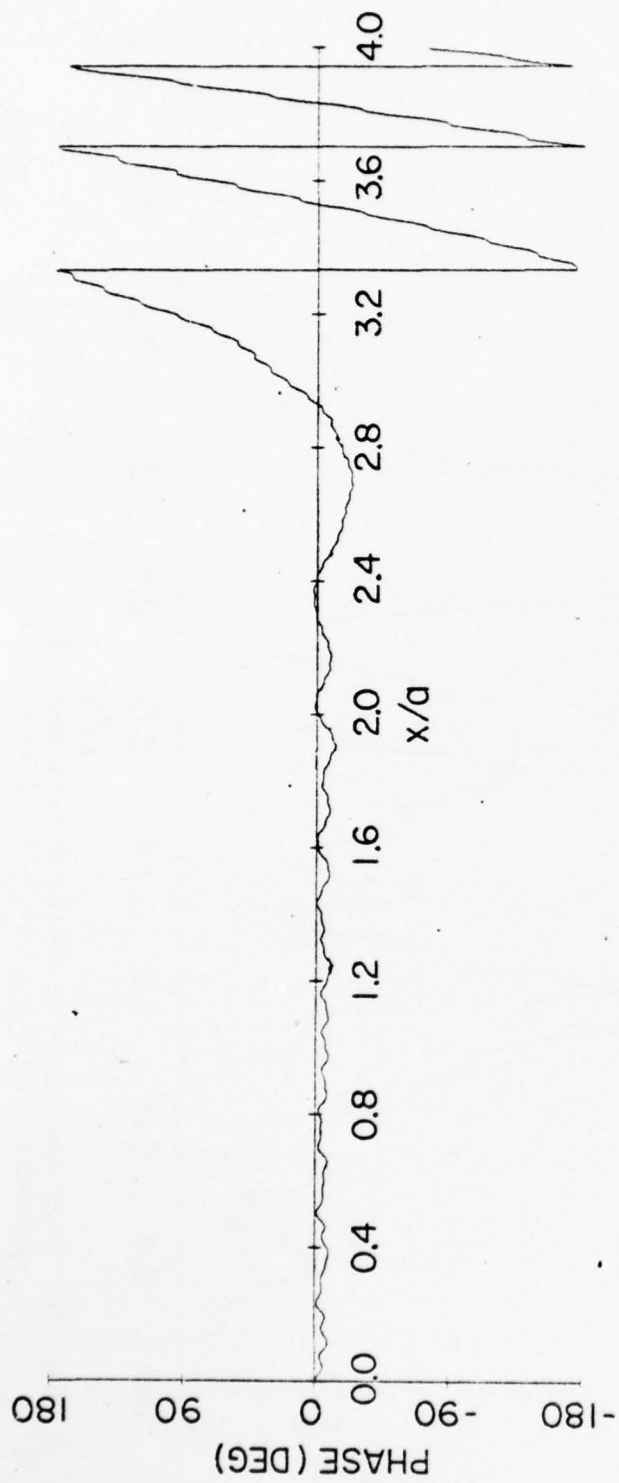Fig. 19.a.   Modulus of λ vs. effective Fresnel number for M = 2.0, symmetric roots.   Bare resonator
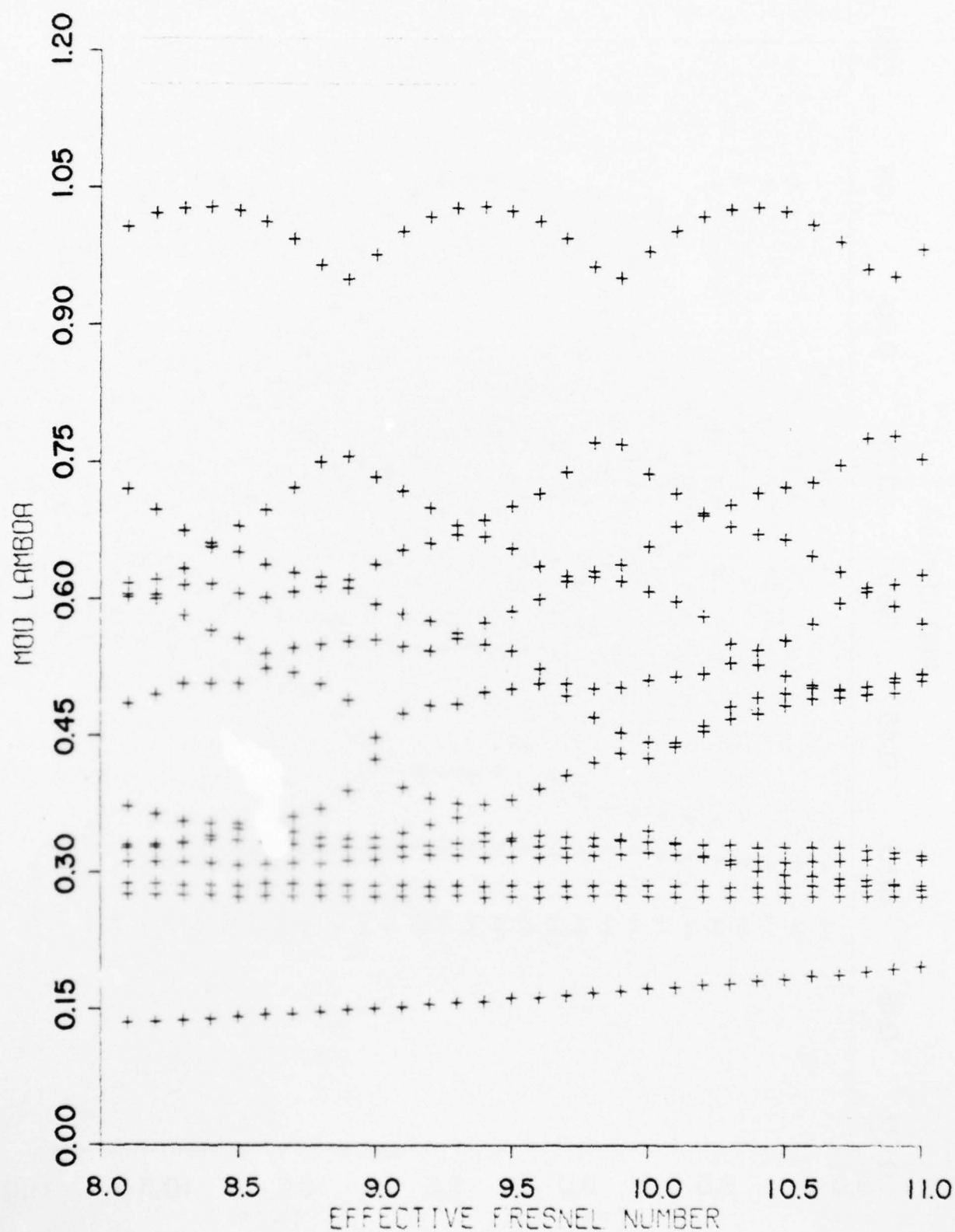
78

Fig. 19.b. Modulus of λ vs. effective Fresnel number for M = 2.0, symmetric roots. Resonator containing Gaussian gain distribution.

79
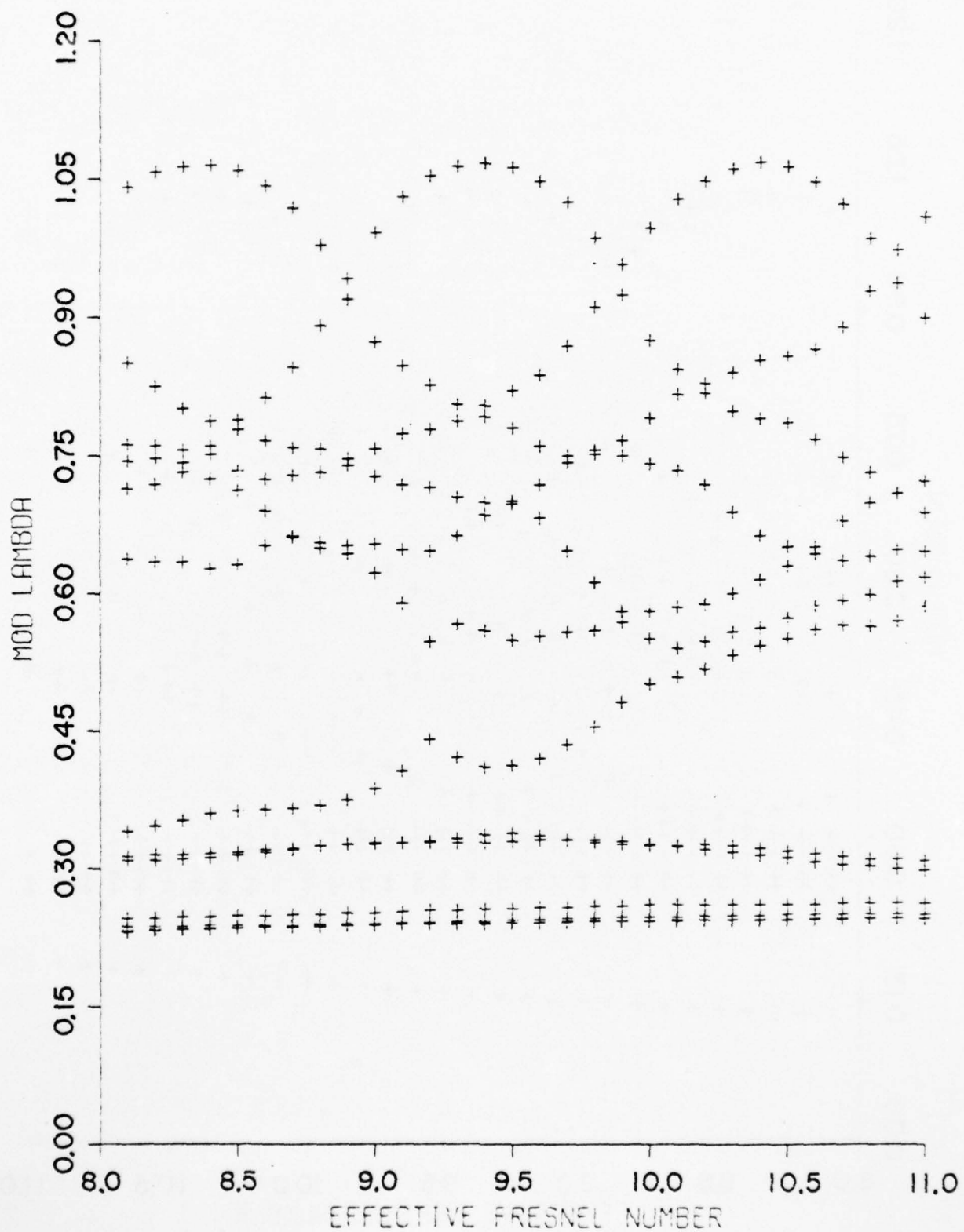
Fig. 19.c. Modulus of λ vs. effective Fresnel number for M = 2.0, symmetric roots. Resonator containing negative Gaussian gain distribution
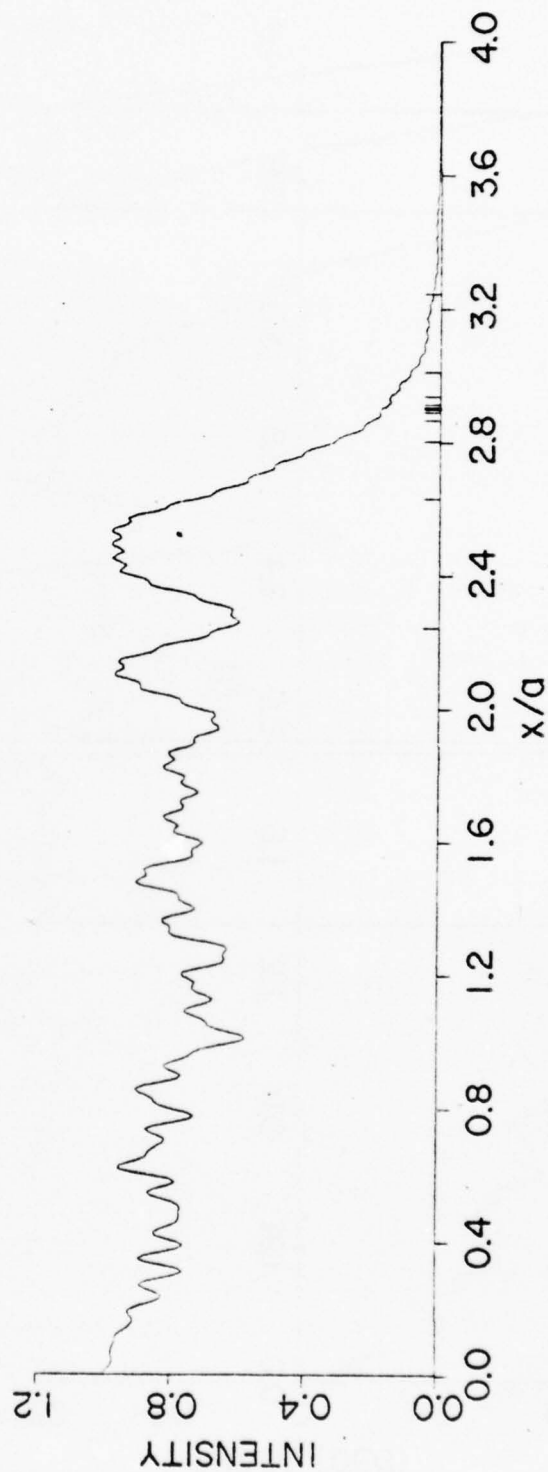
Fig. 20. Phase and intensity of the lowest-loss mode of a bare resonator, for $F_{eff} = 16.4$, $M = 2.9$, $\mu = 0.96145 - 0.004270i$.

81
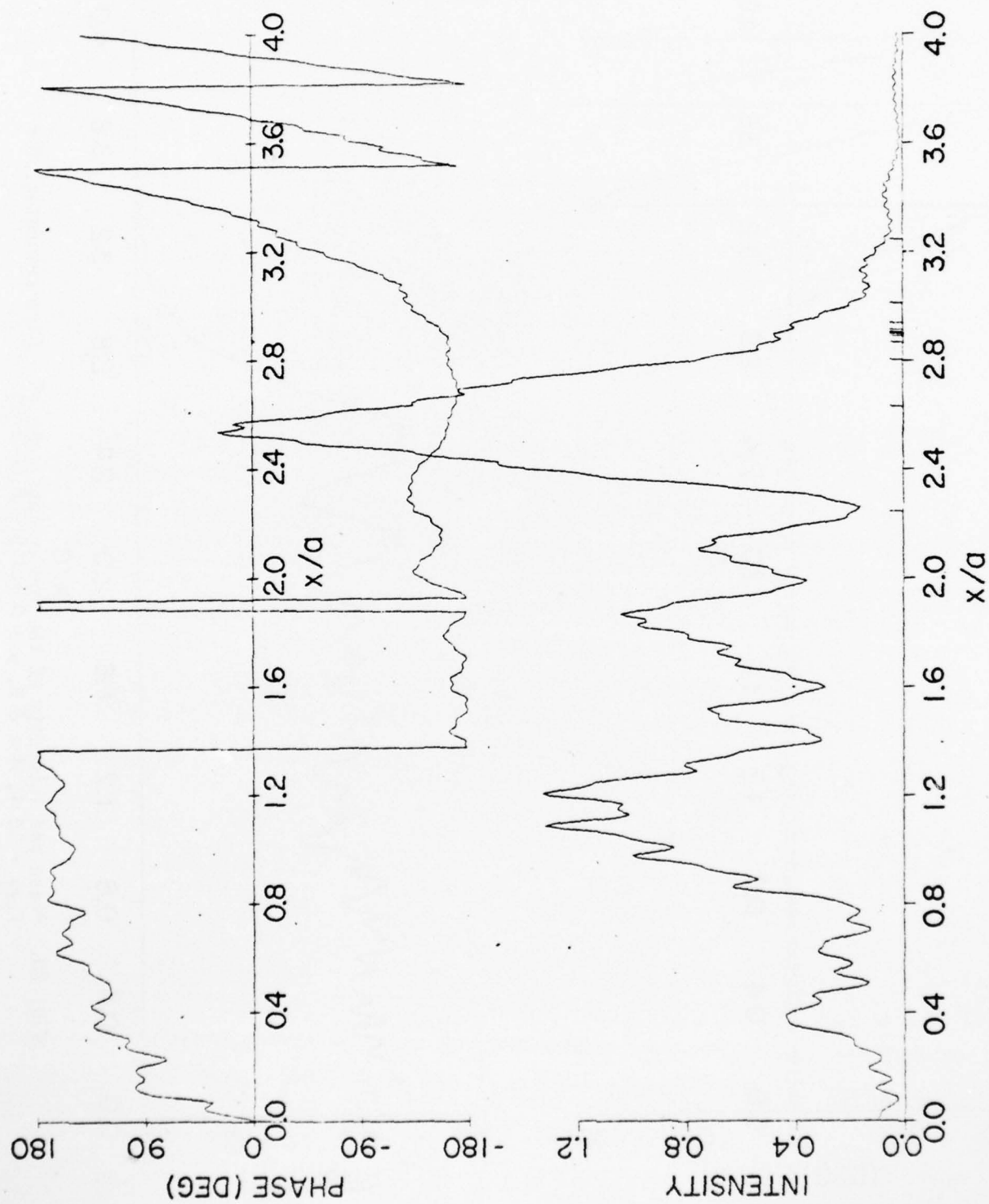
Fig. 21. Phase and intensity of the next-to-lowest-loss symmetric mode of a base resonator, for $F_{eff} = 16.4$, $M = 2.9$, $\mu = 1.1001 + 1.1593i$
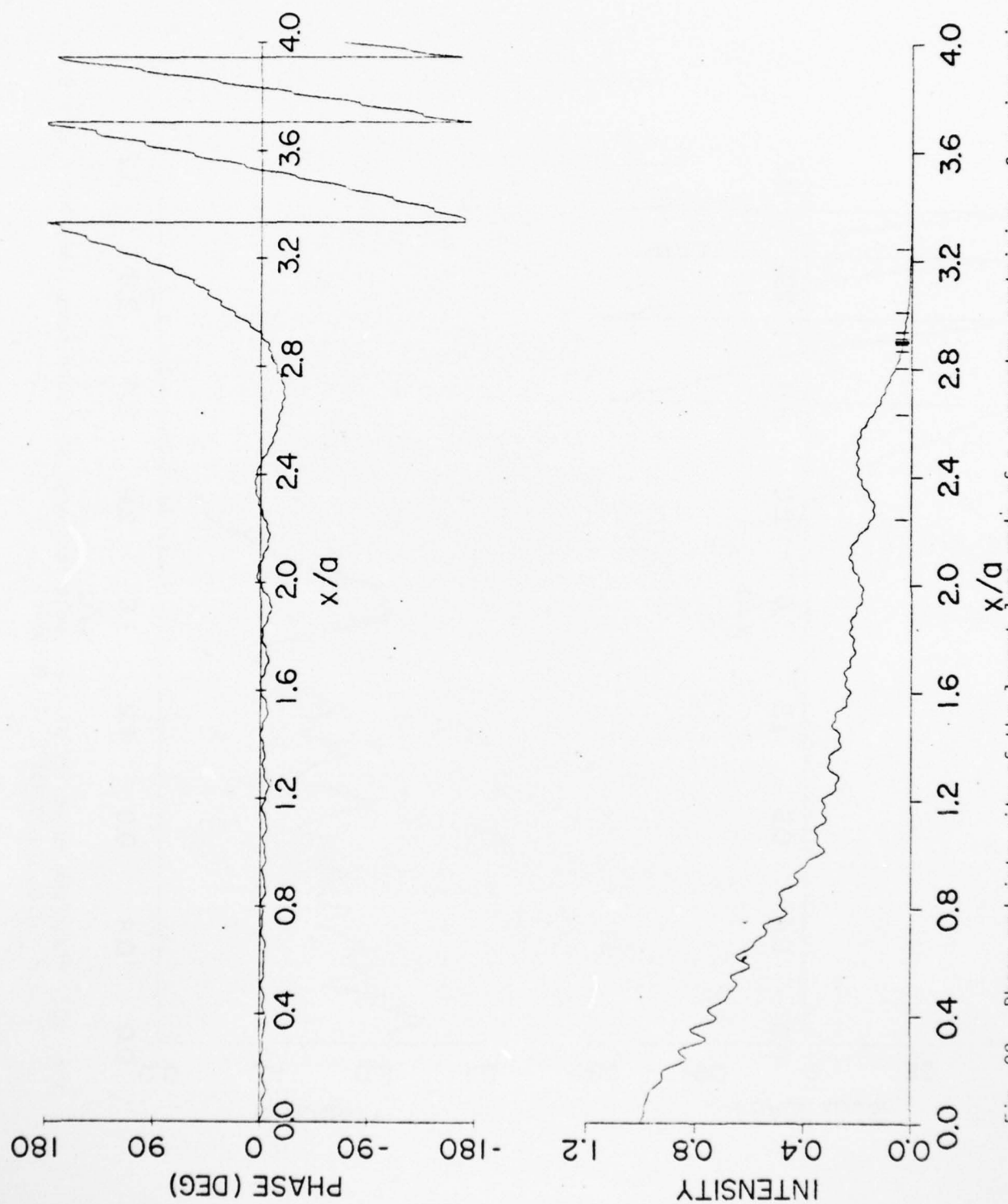
Fig. 22. Phase and intensity of the lowest-loss mode of a resonator containing a Gaussian gain distribution, for $F_{eff} = 16.4$, $M = 2.9$, $\mu = 0.97999 - 0.0028037i$

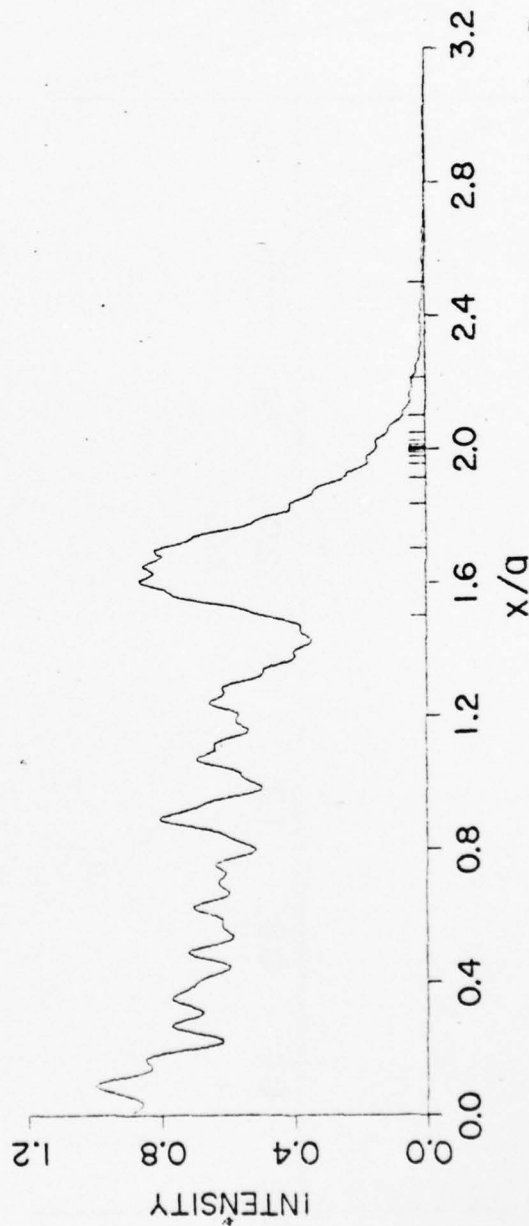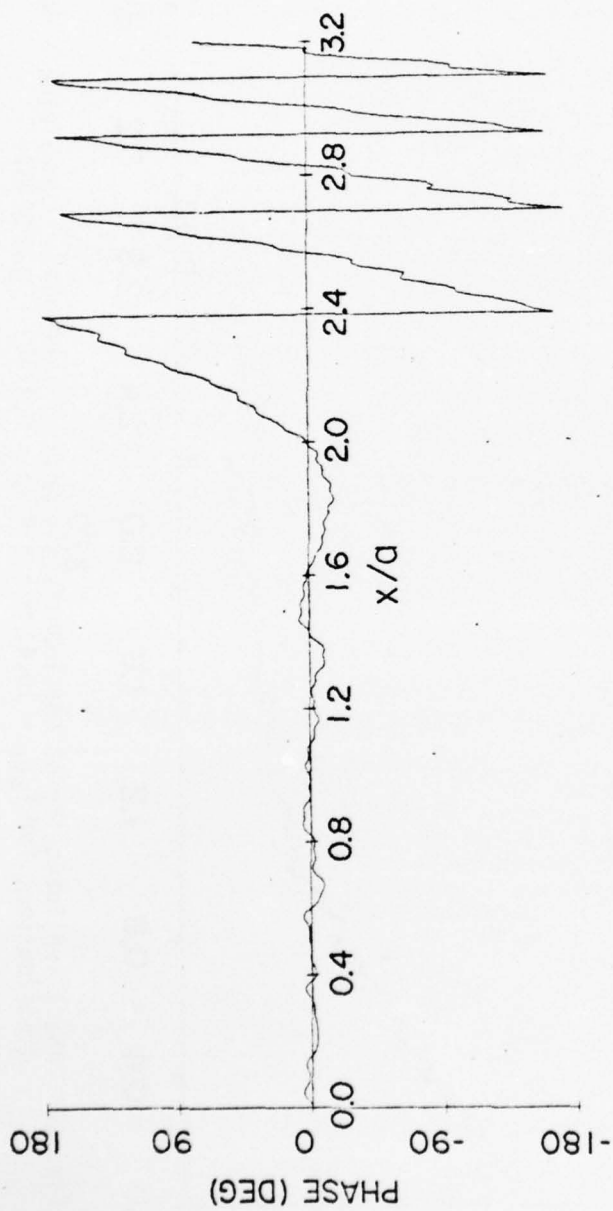Fig. 23. Phase and intensity of the lowest-loss mode of a bare resonator, for $F_{eff} = 8.4$, $M = 2.0$, $\mu = 0.95172 - 0.0060246i$
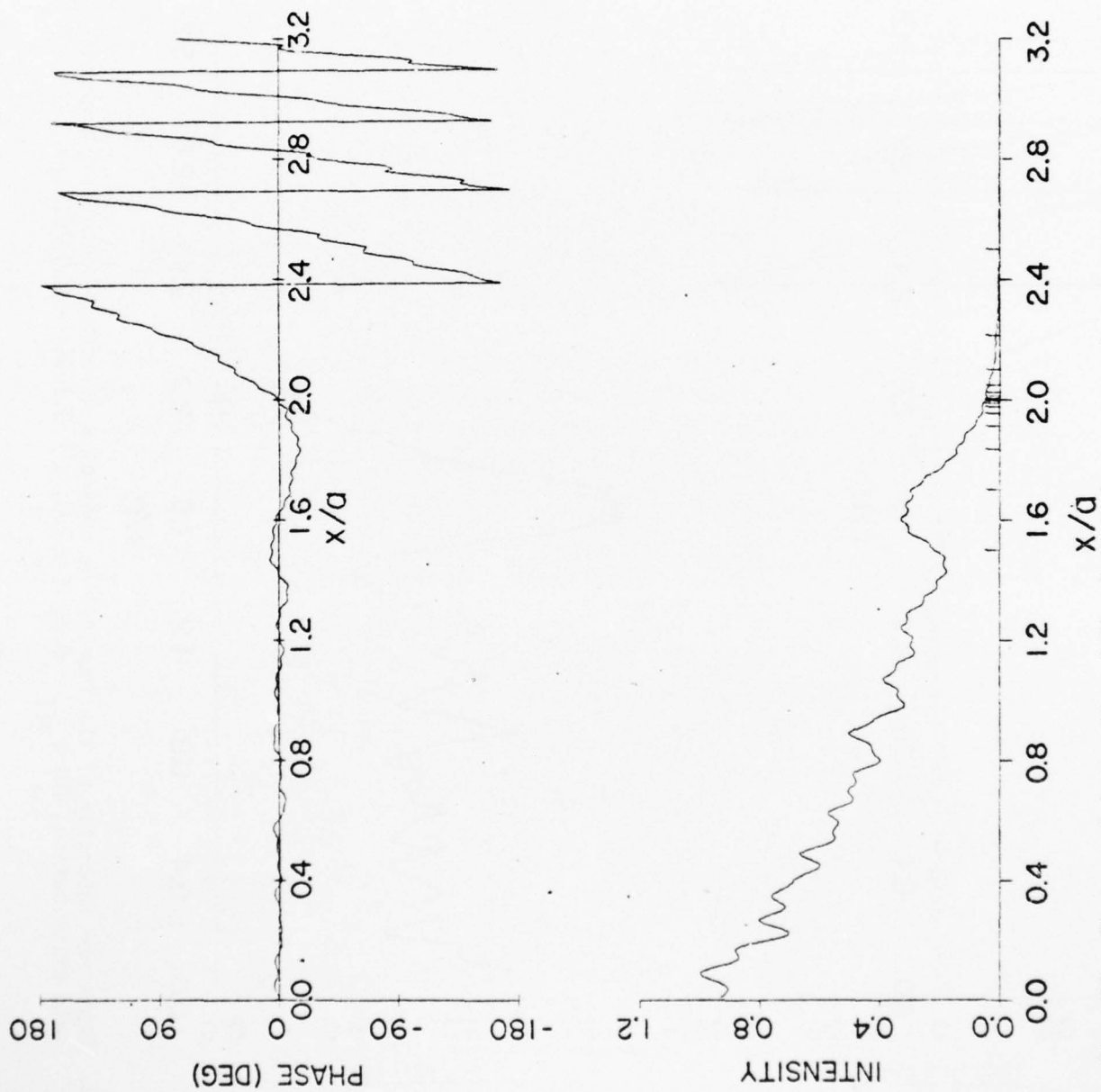
Fig. 24. Phase and intensity of the lowest-loss mode of a resonator containing a Gaussian gain distribution, for $F_{eff} = 8.4$, $M = 2.0$, $\mu = 0.9716 - 0.0038815i$

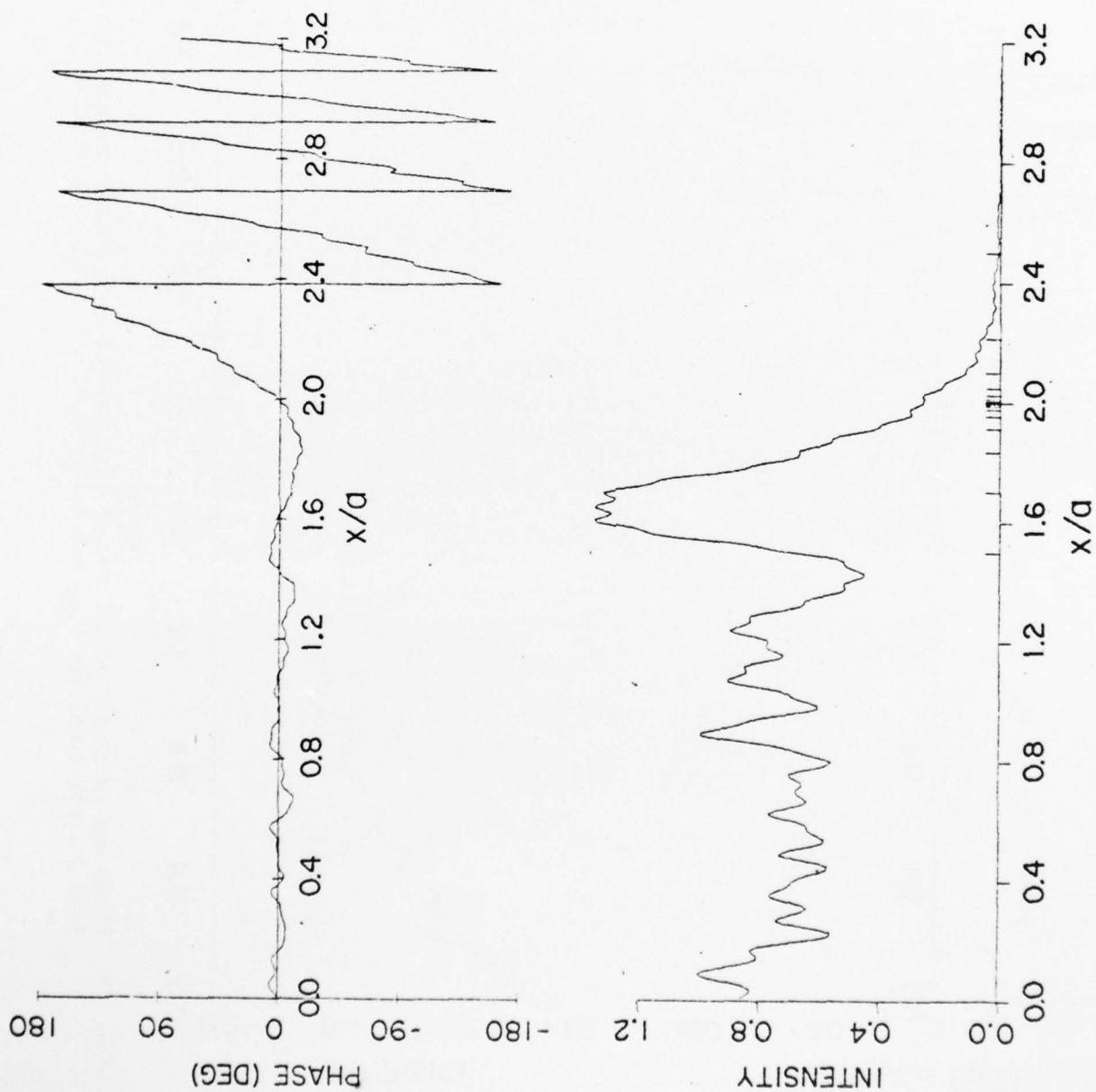Fig. 25. Phase and intensity of the lowest-loss mode of a resonator containing a negative Gaussian gain distribution, for $F_{eff} = 8.4$, $M = 2.0$, $\mu = 0.93869 - 0.0072124i$

REFERENCES

1. P. Horwitz, "Asymptotic theory of unstable resonator modes," J. Opt. Soc. Am. 63, 1528-1543 (1973).

2. A. E. Siegman and E. A. Sziklas, "Mode calculations in unstable resonators with flowing saturable gain. 1: Hermite-Gaussian expansion," Appl. Opt. 13, 2775-2792 (1974).

3. E. A. Sziklas and A. E. Siegman, "Mode calculations in unstable resonator with flowing saturable gain. 2: Fast Fourier transform method," Appl. Opt. 14, 1874-1889 (1975).

4. A. E. Siegman, "Unstable optical resonators," Appl. Opt. 13, 353-367 (1974). This article gives an extensive review of work on unstable resonators prior to 1974.

5. A. E. Siegman, "Unstable optical resonators for laser applications," Proc. IEEE 53, 277-287 (1965).

6. W. W. Rigrod, "Saturation effects in high-gain lasers," J. Appl. Phys. 36, 2487-2490 (1965).

7. G. L. McAllister, W. H. Steier, and W. B. Lacine, "Improved mode properties of unstable resonators with tapered reflectivity mirrors and shaped apertures," IEEE J. Quantum Electron. QE-10, 346-355 (1974).

8. A. Yariv and P. Yeh, "Confinement and stability in optical resonators employing mirrors with Gaussian reflectivity tapers," (to be published).